Energy & Buildings 325 (2024) 114999

Contents lists available at ScienceDirect

Energy & Buildings

journal homepage: www.elsevier.com/locate/enb

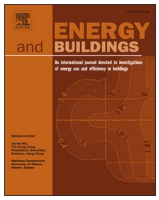

Building performance optimization through sensitivity Analysis, and economic insights using AI

Haidar Hosamo [a,*], Guilherme B. A. Coelho [a,b], Christian Nordahl Rolfsen [a], Dimitrios Kraniotis [a]

[a] Department of Built Environment, Faculty of Technology, Art and Design, Oslo Metropolitan University, PO box 4 St. Olavs plass, Oslo, NO-0130, Norway
[b] CERIS and Departamento de Engenharia Civil, Faculdade de Ciências e Tecnologia, Universidade NOVA de Lisboa, 2829-516 Caparica, Portugal

ARTICLE INFO

Keywords:
Optimizing building designs
Energy efficiency
Thermal comfort
Machine learning techniques
Sensitivity analysis
Economic impact analysis
Building Management System (BMS)

ABSTRACT

Optimizing building designs for energy efficiency and occupant comfort presents significant challenges due to the complex and often conflicting requirements of various stakeholders. Consequently, this study conducts a multifaceted sensitivity and economic impact analysis that aims to improve building performance in terms of energy efficiency and occupant comfort by implementing machine learning techniques. Using a broad dataset comprising of 12,000 energy simulation runs for Tvedestrand Upper Secondary School in Norway, several machine learning models were employed with Multi-Layer Perceptron outperforming the others. In addition, several sensitivity analysis methods were used to explore the influence of individual parameters on building performance. The analysis reveals that ventilation rate, room depth, U-value of the facade, and heat gains significantly affect energy consumption. Economic impact analysis was also carried out to compare the cost-effectiveness of traditional HVAC systems with Building Management System (BMS) HVAC solutions. The BMS HVAC system shows significantly lower operational costs over time, with investment costs averaging around 1200 Norwegian kroner (NOK)/m^2 and operational costs of approximately 150 NOK/m^2 per year. Sensitivity analysis under different economic scenarios highlights the economic viability of the BMS HVAC system. This study identifies optimal building parameters that balance energy efficiency and thermal comfort, achieving total energy consumption between 11.05 and 22.51 kWh/m^2 and zero discomfort hours (h $>$ 26 °C). In sum, the findings offer valuable insights for stakeholders, enabling informed decisions about sustainable building design and energy efficiency improvements, ensuring both technical soundness and financial viability under a wide range of conditions, while using the tested tools.

1. 1.Introduction

1.1. Background

Optimizing building designs for energy efficiency is a critical challenge in the field of sustainable architecture and environmental engineering [1]. Buildings are responsible for a significant portion of global energy consumption, contributing to approximately 40 % of total energy use and associated greenhouse gas emissions worldwide [2 3]. This has profound implications for environmental sustainability and for economic as well as social aspects, as energy-efficient buildings can reduce operational costs and improve occupant health and productivity [4 5 6].

Moreover, achieving optimal thermal comfort is essential as it directly affects the well-being and satisfaction of building occupants [7]. However, balancing these objectives can become rather complex due to the diverse and often conflicting requirements involved. For instance, strategies that maximize energy efficiency, such as minimizing window areas to reduce heat loss, can adversely affect indoor environmental quality and occupant comfort, in this case, which will lead to the reduction of daylight, which, as it is known, is directly connected to occupant visual comfort [8]. Conversely, enhancing natural light to improve occupant satisfaction, by for example, increasing the window size in relation to the floor air, can increase thermal loads and energy consumption for cooling since during the summer season solar gain will increase, which is contradictory to energy efficiency or the reduction of the energy consumption.

Current literature emphasizes the integration of Building Information Modeling (BIM) and advanced computational techniques, like machine learning, to address these challenges [9 10 11 12]. BIM facilitates the detailed modeling and simulation of building performance under

* Corresponding author.
E-mail address: haidarho@oslomet.no (H. Hosamo).

https://doi.org/10.1016/j.enbuild.2024.114999
Received 26 August 2024; Received in revised form 24 October 2024; Accepted 3 November 2024
Available online 6 November 2024

various scenarios, while machine learning offers powerful tools to predict and optimize complex systems. The connection between these two sorts of tools offers both great flexibility in the applied procedure, while providing precise comprehensive results. Despite these advancements, the sensitivity of multi-objective optimizations (MOO) to various input parameters remains underexplored, which Table 1. Most studies focus on the outcomes of optimization techniques without adequately addressing how changes in input parameters influence these outcomes.

Table 1 provides an overview of significant research that integrates machine learning techniques for building energy optimization. It highlights the methodologies and key findings of each study, with a focus on their relevance to the identified gap in sensitivity analysis within multi-objective optimizations. From the results gathered in Table 1 it is visible that there is a need for a comprehensive investigation into how input parameter variations affect the optimization outcomes. This is a literature gap that this study aims to thoroughly address.

Table 1
Summary of Key Studies on BIM and Machine Learning Integration in Building Energy Optimization.

Study Reference	Methodology Used	Key Findings	Relevance to Gap
[13]	BIM and support vector machine (SVM) for predicting building energy consumption	Developed a prediction model for energy consumption using SVM, validated with a teaching building.	Did not explore the sensitivity of input parameters on optimization outcomes.
[14]	Machine Learning with As-Built BIM models in renovation projects	Used Decision Trees and Rule-Based Classification to analyze BIM data for energy renovation decisions.	Focused on decision-making in renovations but lacked sensitivity analysis of the parameters.
[15]	Review of BIM in building performance improvements	Discussed potential of BIM in enhancing energy efficiency and indoor environmental quality.	Did not address sensitivity analysis in the optimization process.
[16]	BIM-based HVAC optimization using Genetic algorithm (GA)	Optimized HVAC control schedules for energy performance.	Lacked a comprehensive sensitivity analysis of variable interactions.
[17]	Interpretable ML for building energy management	Developed a methodology to evaluate Generalized Linear Models (GLM), multi-layer perceptron (MLP), Extreme Gradient Boosting Trees (XGB), and Random Forests (RF) models in building energy management.	Provides a framework for understanding ML predictions but does not focus on sensitivity analysis.
[18]	BIM-based multi-objective optimization using MOO algorithms	Enabled exploration of design alternatives for energy performance optimization.	Methodology focuses on optimization but not on sensitivity of the outcomes to parameter changes.
[19]	BIM for lifecycle energy efficiency	Demonstrated a data-driven approach like MLP and XGB to optimize building lifecycle energy efficiency.	Did not address sensitivity analysis in lifecycle assessment.
[20]	ML-based modeling of building energy systems	Explored the potential of data-driven ML models like MLP, SVM, and RF for energy system modeling.	Focuses on modeling rather than sensitivity analysis of the energy systems.
[21]	BIM for energy demand calculation and simulation	Discussed interoperability issues in BIM to Building Energy Modeling (BEM) applications.	Lacks a focus on the sensitivity of design parameters affecting energy simulations.
[22]	BIM-based low-carbon building design optimization	Used an improved genetic algorithm for optimizing building performance.	Optimizes for low-carbon designs but does not examine the sensitivity of parameter changes.

In addition, this study focusses on studies that integrated BIM with ML since this study aims to develop and extend the work presented in our previous paper [7]. That earlier study combined BIM and ML and the non-dominated sorting genetic algorithm-II (NSGA II) to optimize building energy consumption and thermal comfort. In this study, we aim to perform a multifaceted sensitivity and economic impact analysis that aims to improve building performance in terms of energy efficiency and occupant thermal comfort by implementing machine learning techniques and rendering the building parameters. In addition, this study also tests and shows the performance of several tools of machine learning and sensitivity analysis in terms of building performance optimization. These can be later on used as a guide for selecting the tools to use in future optimization procedures.

1.2. Sensitivity analysis

The complexity of building design is increasing, necessitating a multifaceted approach involving various stakeholders who must adhere to strict regulations within constrained budgets. Building performance simulation (BPS) software, such as IDA Indoor Climate and Energy (IDA ICE) [23 24] and EnergyPlus [25], plays an important role in assisting decision-makers to identify designs that ensure a comfortable and healthy indoor environment while minimizing environmental impact and costs [26].

IDA ICE and EnergyPlus are widely used in the field of energy performance modeling. Although both tools are capable of performing detailed energy simulations, they have key differences and similarities, as outlined in Table 2. For instance, IDA ICE uses symbolic equations and is highly suited for complex energy behavior, such as phase change materials (PCM) and their hysteresis effects, providing higher accuracy in these areas [25]. However, it has less flexibility in external convective heat transfer modeling compared to EnergyPlus. On the other hand, EnergyPlus is known for its modular structure and adaptive convection algorithms, offering detailed optical and solar radiation models, but lacks the ability to simulate PCM hysteresis [25].

The design team typically manipulates a broad array of parameters,

Table 2
Comparison of IDA ICE and EnergyPlus.

Feature	IDA ICE	EnergyPlus
Interface	User-friendly, graphical	Text-based, command-line or GUI
Flexibility	Predefined components for HVAC	Highly customizable with scripting
HVAC Modeling	Detailed built-in HVAC simulation	Requires more custom configurations
Dynamic Simulation Capabilities	Strong focus on indoor climate and HVAC operations	Focuses on energy performance and envelope modeling
Custom Controls	Limited customization	Highly flexible with custom control strategies
PCM (Phase Change Material) Modeling	Supports hysteresis modeling for PCM behavior	Does not support PCM hysteresis, simpler radiation models
Convective Heat Transfer	Less flexible in external convective heat transfer	Offers adaptive convection algorithms
Optical Models	Basic optical models	Detailed optical and solar radiation models
Common Use	Detailed thermal comfort and HVAC system simulation	Custom energy performance models

including window-wall ratio, glazing properties, ventilation rates, and insulation levels, among many others aspects [27]. These parameters create an extensive multi-dimensional design space that needs to be thoroughly explored to uncover viable solutions that satisfy all stakeholder expectations and goals. The methodologies for exploring this vast array of opportunities vary significantly across different countries, companies, and practitioners [28 29], largely influenced by the capabilities of the employed software to handle parameter variations and perform optimizations [30 31 32].

One-at-a-time (OAT) variations are a widely used method in the exploration of design space where a single parameter is adjusted while others remain fixed, allowing designers to isolate the effects of individual variables [33 34]. This methodical approach facilitates a clearer understanding of each parameter's influence on the overall system performance by sequentially testing the impact of changing one variable at a time through successive simulations. OAT variations are particularly valued for their simplicity and the direct insights they provide, which can be crucial in the early stages of design development. Despite its straightforward nature, the effectiveness of OAT in providing comprehensive solutions is limited, as it often focuses on local rather than global optimization, potentially overlooking interactions between parameters that could lead to more innovative and effective designs.

Conducting these parameter studies manually is a difficult process that requires methodical attention to detail to prevent errors. Due to time constraints, a modeler might only adjust a few critical parameters, which may not always align with those identified as most impactful through quantitative sensitivity analysis [35]. This mismatch can limit the effectiveness of the parameter study in achieving optimal designs. Automating simulations allows for the inclusion of more variables and enables rapid OAT variations, such as using sliders in visual programming or using python [36 37]. However, while useful, OAT methods typically only uncover local optima within specific areas of the design space. To comprehensively explore and identify globally optimal designs across the multidimensional space, the adoption of "global" exploration methods is essential [38].

This integration of both local and global optimization strategies allows for a more holistic approach to design exploration, enhancing the potential for discovering innovative solutions that meet broader performance criteria [39]. Implementing advanced statistical and computational techniques such as Monte Carlo simulation (MCS) [40] and Partial Rank Correlation Coefficient (PRCC) [41] can further refine the exploration process. MCS is a robust technique used to model the probability of different outcomes by performing random sampling of input parameter [42 43]. In building performance analysis, MCS is instrumental in evaluating how variations in parameters influence key metrics such as thermal comfort [44] and energy consumption [45]. MCS provides a comprehensive understanding of the potential outcomes and interactions among parameters, by simulating numerous scenarios with randomly sampled parameter values [46]. Østergård et al. used Monte Carlo simulations to evaluate the energy demand and thermal comfort of an office room, involving 93,750 design combinations. The performance was assessed based on energy demand and the number of hours exceeding a thermal comfort threshold of 26 °C (h $>$ 26 °C), demonstrating the robustness of Monte Carlo methods in optimizing building performance [38].

These techniques share a common feature where they simultaneously vary multiple inputs to account for parameter interactions and comprehensively cover the combined design space and enable a deeper analysis of the interactions between multiple variables, revealing complex dependencies and synergies that single-parameter studies might miss which is the focus of this study.

1.3. Economic impact analysis in context

Economic impact analysis is an important aspect of building performance studies, as it helps stakeholders understand the financial implications of various design and operational strategies [47]. While many studies have explored the economic benefits of energy-efficient building practices [48 1 49 50], the integration of comprehensive sensitivity analysis into these economic evaluations is often overlooked.

Economic evaluations in building performance research typically focus on cost-benefit analyses [51], payback periods [52], net present value (NPV) [53], and return on investment (ROI) [54] for various energy-saving measures. For instance, studies have shown that investments in high-efficiency insulation [55] and energy-efficient windows [56] can lead to significant long-term savings by reducing energy consumption and improving thermal comfort.

However, the economic analyses in these studies often rely on static assumptions about building performance parameters. They usually do not account for the variability and uncertainty associated with these parameters, which can significantly influence the economic outcomes. For example, the payback period for installing solar panels may vary widely depending on factors such as local climate conditions, electricity prices, and government incentives. Without considering these variations, the economic assessments may provide an incomplete or overly optimistic view of the financial viability of energy-saving measures.

Sensitivity analysis can enhance economic evaluations by accounting for the uncertainties and interactions between different building performance parameters [57]. Sensitivity analysis provides strong understanding of the potential risks and benefits associated with energy-efficient building strategies by systematically varying key inputs and assessing their impact on economic outcomes [58].

Previous studies that have incorporated sensitivity analysis into their economic evaluations typically use methods such as Monte Carlo simulations, which allow for the exploration of a wide range of scenarios and their probabilistic outcomes [59]. Despite these advancements, many building performance studies still do not fully integrate sensitivity analysis into their economic evaluations. This omission can lead to an underestimation of the economic risks associated with building design and operational decisions.

This study aims to bridge the gap in the literature by integrating a detailed sensitivity analysis into the economic evaluation of building performance parameters. This research provides a thorough examination of how variations in building parameters influence both energy performance and economic outcomes by using OAT sensitivity analysis, PRCC analysis, MCS, and Analysis of Variance (ANOVA) [60].

1.4. Research gap and the scope of the work

This research aims to address the critical gap of understanding the stability and robustness of optimization solutions in building performance by conducting a detailed sensitivity analysis. The database developed in authors previous work [7] will be employed and extend it.

The previous paper integrates Building Information Modeling (BIM) with machine learning (ML) and the non-dominated sorting genetic algorithm-II (NSGA II) to optimize building energy consumption and thermal comfort, focusing on the use of IDA Indoor Climate and Energy (IDA ICE). The dataset for machine learning models was generated using pairwise testing, initially producing 8,000 combinations of building parameters following by 8,000 simulations in IDA ICE to obtain the energy and comfort results. In this study, the dataset was extended by 4,000 new simulations to reach 12,000 combinations to investigate the accuracy of the model. This was inspired by the work done by [38]. Using 4 laptops, it took approximately 21 days to complete all 12,000 simulations.

Despite the significant advancements in machine learning (ML) for optimizing building energy consumption and thermal comfort, critical gaps remain in the field. Specifically, there is a lack of comprehensive understanding of how variations in input parameters influence the optimization outcomes. Existing studies predominantly emphasize the results of optimization techniques without adequately exploring the sensitivity of these results to changes in input parameters (Table 1).

Additionally, the robustness and economic feasibility of these optimization solutions in real-world applications have not been thoroughly investigated.

The novelty of this work is highlighted by its multifaceted approach to sensitivity analysis and economic evaluation within building performance prediction. This study employs a wide range of machine learning models, including Linear Regression (LR), Random Forest (RF), Support Vector Regression (SVR), Decision Tree (DT), Extreme Gradient Boosting (XGBoost), and Multi-Layer Perceptron (MLP). This research offers a thorough examination of parameter impacts by integrating this with various sensitivity analysis methods such as OAT sensitivity analysis, PRCC analysis, Monte Carlo simulations, and ANOVA.

The economic analysis in this study provides scenario-based evaluations and the Norwegian price book financial model [61] and NS-EN 15459–1:2017 [62] to assess the viability of various energy-saving strategies in the Norwegian context. Hence, this study identifies the most influential building parameters and evaluates the robustness and economic feasibility of different energy-saving solutions. This approach ensures that the proposed strategies are technically sound and financially viable under a wide range of conditions, providing valuable insights for stakeholders in making informed decisions about sustainable building design and energy efficiency improvements.

2. Methodology

The methodology of this research, as can be seen in Fig. 1, begins with the collection of a substantial dataset generated from 12,000 simulation runs in IDA ICE, covering a wide range of building parameters and performance metrics. Following data collection, a comprehensive data preparation process is carried out, which includes structuring of the data to ensure it is suitable for machine learning models. This prepared dataset is then used as input for various machine learning models, such as Linear Regression, Random Forest, SVR, Decision Tree, XGBoost, and MLP, to predict and analyze building performance with high accuracy as possible. Additionally, the work in this paper incorporates sensitivity analysis to identify the most influential design parameters on building performance. It also evaluates the economic impacts of different HVAC systems, comparing traditional HVAC solutions with Building Management Systems (BMS) [37] solutions to highlight the cost-effectiveness of the latter.

2.1. Database collection and preparation

The case study for this research is based on Tvedestrand Upper Secondary School, located in Tvedestrand, Norway (Fig. 2) [63 7]. Built in 2020, this school serves as the baseline for the simulations and represents educational facilities in Norway. The building is a three-story structure with a total floor area of 14,500 m^2, designed to accommodate 690 students and 140 employees.

Its construction complies with the Norwegian building code TEK10 [64] and aligns with the NS3701 standard [65], which sets criteria for passive houses and low-energy commercial buildings. Table 3 outlines the key building parameters used in the baseline simulation, including U-values for the external walls, roof, and windows. The building also features vertical fins on the windows for shading, contributing to reduced solar heat gains. The mechanical balanced ventilation system operates with an 85 % rotary heat recovery efficiency, ensuring minimal energy loss in the ventilation process.

Internal heat gains, occupancy patterns, and energy loads are modelled in accordance with the NS3031 standard [66], which is still referenced in building regulations to simulate realistic performance under Norwegian climatic conditions. The HVAC systems, equipped with rotary heat exchangers, bypass mechanisms, heaters, and chillers, service various functional areas, such as conference rooms, classrooms, and offices, ensuring efficient temperature regulation throughout the building.

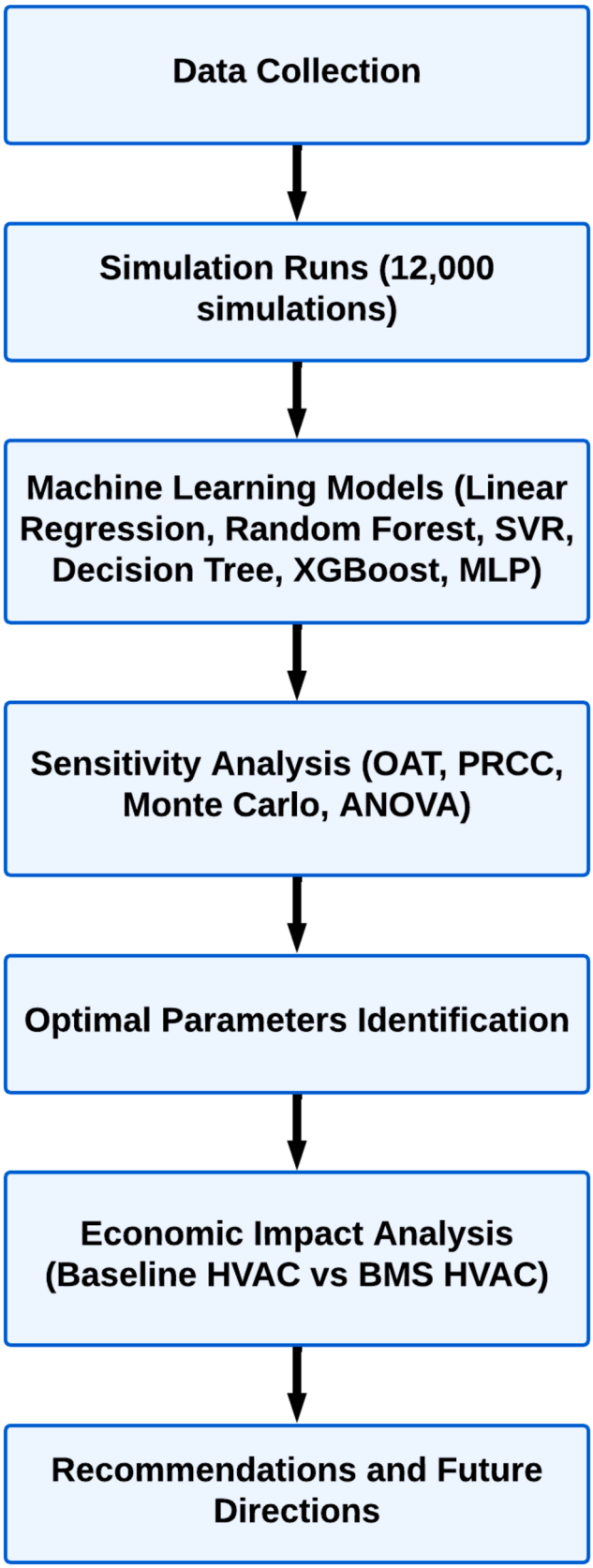

Fig. 1. The methodology framework for predictive analysis and optimization of building performance using machine learning and sensitivity analysis.

Fig. 2. Location and 3D model of Tvedestrand Upper Secondary School (Tvedestrand VGS): (a) Google Map showing the school's location, (b) 3D architectural model of the school building [36].

Table 3
The initial building parameters used in the simulations for the baseline case study building.

Parameter	Initial Value
External wall U-value (W/(m^2·K))	0.15
Roof U-value (W/(m^2·K))	0.11
Window U-value (W/(m^2·K))	0.8
Ground floor U-value (W/(m^2·K))	0.06
Thermal bridge U-value (W/(m^2·K))	0.03
Airtightness (1/h)	0.35
Window-to-Wall Ratio (WWR)	40 %
Shading factor	0.2
Reflectance	0.55
Ventilation system	Mechanical balanced with rotary heat recovery (85 % efficiency)
Specific Fan Power (SFP) (kW/(l/s))	1.4
Ventilation airflow (l/(m^2·s))	2.48 (occupied), 0.81 (unoccupied)
Room heating system	Centralized heating system, 90 % efficiency
Room cooling system	Centralized water cooling for AHU supply air
Heating setpoint (°C)	21
Cooling setpoint (°C)	24
Lighting power (W/m^2)	5.03
Occupancy (W/person)	108
Energy consumption (kWh/m^2·year)	61.07

The dataset generated for this study consists of 12,000 simulation runs. These simulations were determined through a systematic approach using pairwise tests [67], which allowed efficient exploration of the impact of various combinations of input parameters on building energy performance. Key parameters such as U-values for external walls, window-to-wall ratios (WWR), and ventilation rates were tested to assess their influence on total energy consumption.

This method identified the most sensitive interactions between parameters, ensuring the simulations covered a representative range of scenarios while maintaining computational efficiency. After conducting these pairwise tests, it was concluded that 12,000 runs were sufficient to provide reliable and meaningful insights into the building's energy performance, capturing essential interactions without redundancy.

Fig. 3 and Table 4 provide a statistical presentation of building performance parameters from the dataset. Fig. 3 consists of three plots and Table 4 complements these findings by summarizing key parameters such as mean room depth, U-value for external walls, WWR, g-value, and total energy, providing a clear quantification of the dataset's characteristics, which ranges from small, low-mass rooms to large with varied energy consumption profiles.

2.2. Machine learning models for predictive analysis

In the developed predictive modeling, several machine learning algorithms to identify the one that best fits the database were compared. Linear Regression [68] aims to model the relationship between a scalar response and one or more explanatory variables by fitting a linear equation to observed data. The model is represented by $y = \beta_0 + \beta_1 x_1 + \cdots + \beta_n x_n + \epsilon$ where y is the dependent variable, x_i are the independent variables, β_i are the coefficients, and ϵ is the error term.

Random Forest [69] is an ensemble method that operates by constructing a multitude of decision trees at training time and outputting the mean prediction of the individual trees. A single decision tree is built

Table 4
Summary Table of Key Parameters.

Parameter	Mean	Std Dev	Min	Max
Room depth (m)	5.983177	1.147535	4	8
U-val, façade W/(m^2·K)	0.152566	0.029741	0.12	0.20
WWR %	59.83041	17.26992	30	90
g-value	0.414186	0.134545	0.25	0.63
Overhang (cm)	29.90286	22.39942	0	60
Shading factor	0.496229	0.221191	0.2	0.8
Shade on (lx)	60997.14	20278.15	38,000	100,000
Ventilation rate (min air) (ACH)	1.245726	0.431837	0.5	2
Heat gains W/m^2	17.55756	7.279167	5	30
Lighting W/m^2	5.026286	2.245416	2	8
Reflectance	0.593143	0.13938	0.4	0.78
h > 26 °C (hours)	65.23192	127.9567	0	1140
Total energy (kWh/m^2. year)	48.14413	14.96192	21	100

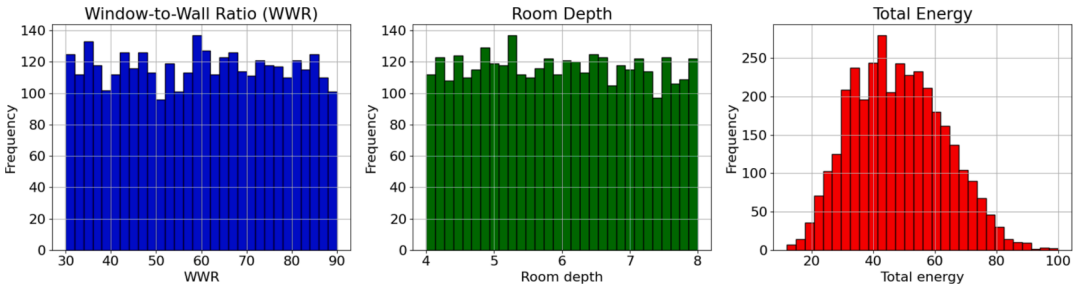

Fig. 3. Example of Comprehensive Visualization of Building Performance Parameters and Total Energy Consumption. Left: The histogram showcases the distribution of WWR within the dataset. Center: the distribution of room depth. Right: total energy consumption.

using the equation $Y = f(X) + \epsilon$ where X is the input variable, Y is the output, and f represents the tree.

Support Vector Regression (SVR) [70] works by mapping the input features into a high-dimensional feature space and finding a hyperplane that best fits the data. The optimization problem can be expressed as minimizing $\frac{1}{2}||w||^2 + C\sum_{i=1}^{n}\xi_i$ subject to $y_i - \langle w, x_i\rangle - b \leq \epsilon + \xi_i$- and $\langle w, x_i\rangle + b - y_i \leq \epsilon + \xi_i$ where: $||w||^2$ is the regularization term to ensure flatness of the function (minimizing model complexity), C is a regularization parameter that controls the trade-off between achieving a low error and a low model complexity, and ξ_i is slack variables, representing the amount by which the prediction error for each data point exceeds the ϵ margin.

Multi-Layer Perceptron (MLP), a class of feedforward artificial neural network (ANN) [71], consists of three layers of nodes: an input layer, a hidden layer, and an output layer. Each node, or artificial neuron, uses a nonlinear activation function which is the sigmoid function here $\sigma(z) = \frac{1}{1+e^{-z}}$ where σ represents the function itself, mapping real-valued inputs into the interval (0, 1); z is the weighted sum of the previous layer's outputs in neural networks; e is the base of the natural logarithm, approximately 2.71828; $-z$ reverses the direction of the exponential function's growth.

Finally, XGBoost is a scalable and accurate implementation of gradient boosting machines [72]. The model is built in a stage-wise fashion as it is an ensemble of weak learners, typically decision trees. For a given loss function L, the objective at step t is to add a function f_t that minimizes $L\left(y, \hat{y}_{t-1} + f_t\right)$ where $\hat{y}_{t-1}$ is the prediction from the previous step.

In implementing the machine learning algorithms for predictive modeling, several Python libraries were employed to ensure robust performance. Scikit-learn [73] was used for algorithms such as Linear Regression, Random Forest, and Support Vector Regression (SVR), as well as for cross-validation. Scikit-learn was also used for the One-at-a-Time (OAT) method and Partial Rank Correlation Coefficient (PRCC) analysis, along with the Monte Carlo Simulations (MCS). The TensorFlow [74] and Keras [75] libraries were utilized to implement the Multi-Layer Perceptron (MLP), while XGBoost package [76] was applied for the XGBoost gradient boosting algorithm. Additionally, NumPy and Pandas [77] facilitated data manipulation and preprocessing, ensuring efficient handling of the dataset, and Matplotlib [78] and Seaborn [79] were used for visualizing the results, such as error distributions and performance metrics.

The results are validated using both Mean Squared Error (MSE) and R-squared (R^2). MSE is a measure of the average squared difference between the observed actual outturns and the values predicted by the model [80]. It quantifies the difference between the predicted and actual values and squares each difference to eliminate any negative signs. MSE is a risk function, corresponding to the expected value of the squared error loss. The equation for MSE is:

$$MSE = \frac{1}{n}\sum_{i=1}^{n}(y_i - \hat{y}_i)^2$$

Where y_i is the actual value and $\hat{y}_i$ is the predicted value from the model, and n is the number of observations.

Moreover, R-squared (R^2) [81], also known as the coefficient of determination, is a statistical measure that represents the proportion of the variance for a dependent variable that's explained by an independent variable or variables in a regression model. It provides a measure of how well observed outcomes are replicated by the model, based on the proportion of total variation of outcomes explained by the model. The equation for R2 is:

$$R^2 = 1 - \frac{\sum_{i=1}^{n}(y_i - \hat{y}_i)^2}{\sum_{i=1}^{n}(y_i - \bar{y})^2}$$

Where $\bar{y}$ is the mean of the observed data. Higher values of R^2 indicate a better fit of the model to the data.

Fig. 4 illustrates the inputs to a machine learning model designed to predict total energy consumption within the building. The diagram identifies different factors, including room depth, U-value of the façade, window-to-wall ratio (WWR), g-value, and others like shading factor and lighting intensity.

To ensure our model selection is robust and our predictive analysis is reliable, cross-validation techniques were employed [82]. Cross-validation allows to test the efficacy of each machine learning model on different subsets of the dataset, thereby mitigating the risk of overfitting and ensuring that the models generalize well to new data. Specifically, k-fold cross-validation were utilized, where the data is split into k different subsets (or folds). Each model is trained on k-1 of these folds, with the remaining fold used as the test set. This process is repeated such that each fold serves as the test set once, allowing us to assess model performance across different slices of the data. The results from these k iterations are then averaged to provide a comprehensive measure of the model's predictive accuracy. This method helps in validating the models and fine-tuning them by comparing their performance across various configurations and tuning parameters (Table 5).

2.3. Sensitivity analysis

2.3.1. One-at-a-Time (OAT) method

The OAT method offers a structured approach to sensitivity analysis by determining the influence of individual model parameters on output. This method is particularly valuable in complex models where interactions among multiple parameters can obscure their individual effects. The OAT method simplifies the analysis by isolating the impact of one parameter at a time, making it easier to identify key parameters that significantly affect model performance.

The analysis begins by setting all parameters to their baseline values (Table 3) that are representative of standard operating conditions and the most common settings under which the system is evaluated. Establishing a consistent baseline is important as it ensures that any variation in output can be directly attributed to the changes made in a single parameter, thereby eliminating confounding influences from other variables.

Each parameter x_i is systematically varied one at a time. The selection process involves determining which parameters are likely to have the most significant impact on the output, based on either prior empirical studies or theoretical considerations. Once selected, the parameter is varied through a predefined range or set of discrete values. This range is carefully chosen to reflect realistic scenarios that might be encountered in actual system operations. The variation of each parameter is mathematically defined as: $\Delta x_i = \alpha\left(x_{i,\max} - x_{i,\min}\right)$ where α is a scaling factor that represents a step size relative to the parameter's total possible range, and $x_{i,\max}$ and $x_{i,\min}$ are the maximum and minimum values the parameter can take, respectively.

For each incremental value Δx_i, the model is run, and the resulting output is recorded. This process involves adjusting the parameter x_i by the increment Δx_i while maintaining all other parameters at their baseline values. The outputs are then documented for each variation to analyse the model's response to changes in the parameter. The specific impact of altering x_i on the output is captured by: $\Delta f = f(x_1, \cdots, x_i + \Delta x_i, \cdots, x_n) - f(x_1, \cdots, x_i, \cdots, x_n)$ where f represents the model's output function. This formula quantifies the change in output due to the modification in the parameter and is central to understanding the sensitivity of the model to changes in x_i.

After analysing one parameter, it is reset to its baseline value, and the next parameter is selected for variation. This cycle is repeated for each parameter in the model, ensuring a comprehensive exploration of the influence of each parameter on the model's output.

To quantify and compare the sensitivity of different parameters, a

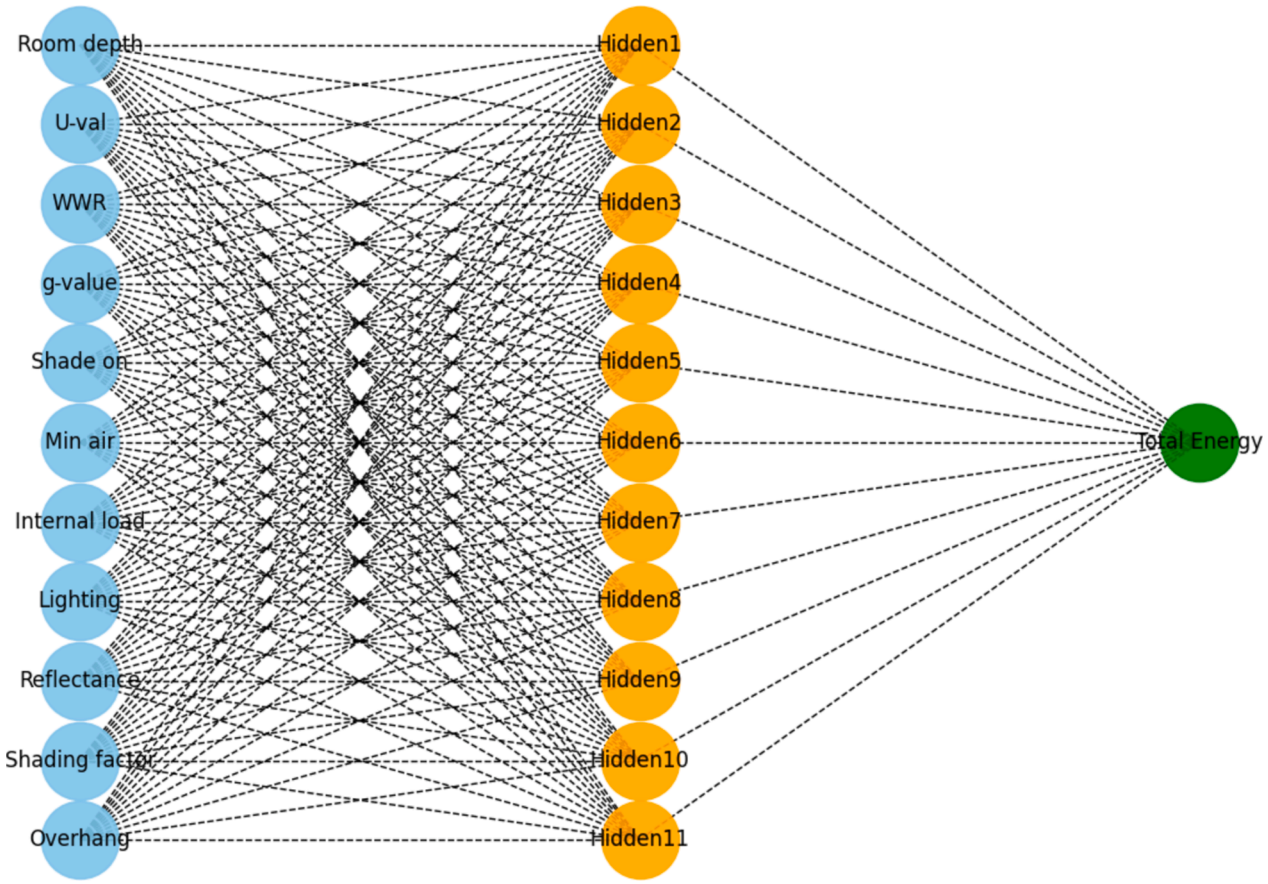

Fig. 4. The 11 inputs used in the machine learning model to predict the output "Total Energy".

Table 5
Hyperparameters optimization results.

Algorithm	Best Hyperparameters
Linear Regression	–
Random Forest	Number of Trees: 100 Maximum Depth: 10 Minimum Samples Split: 2 Minimum Samples Leaf: 1 Bootstrap: True
Support Vector Regression (SVR)	Regularization Parameter (C): 1.0 Epsilon (epsilon): 0.1 Kernel: Radial Basis Function (rbf) Gamma: scale
Multi-Layer Perceptron (MLP)	Hidden Layer Sizes: (11) Activation Function (activation): Rectified Linear Unit (relu) Solver: Adam Alpha: 0.0001
XGBoost	Number of Boosting Rounds: 100 Learning Rate: 0.1 Maximum Depth: 6 Subsample Ratio: 0.8 Colsample by Tree: 0.8

sensitivity index S_i can be calculated as follows: $S_i = \frac{\Delta f}{\Delta x_i}$. This index normalizes the output change relative to the size of the parameter change, providing a standardized measure of sensitivity across all parameters. Furthermore, if variability and uncertainty are significant factors, an aggregate sensitivity measure can be derived from multiple runs or scenarios using $S_{i,total} = \sum_{j=1}^{N} \left| \frac{\Delta f_j}{\Delta x_{i,j}} \right|$ where N is the number of tests or simulations conducted.

2.3.2. Partial Rank correlation coefficient (PRCC)

The PRCC analysis plays a pivotal role in our study, enabling the systematic identification and prioritization of influential parameters within complex predictive models. PRCC is particularly suited for models characterized by non-linear relationships and the intricate interplay among multiple variables. This method assesses the strength and directional associations between individual model parameters and the output while controlling for the effects of other interrelated variables, thereby isolating the specific impact of each parameter.

The process begins by setting all model parameters to their baseline values, ensuring a controlled and consistent starting point for the sensitivity analysis. PRCC analysis is then conducted across a range of carefully chosen variations for each parameter. This strategic variation allows us to control for the confounding effects of parameter interdependencies and to accurately gauge the influence of each parameter on model output.

PRCC calculates rank correlation coefficients, which are robust against non-normal data distributions and ideal for non-linear data analysis scenarios. The PRCC for a parameter x_i relative to the output y can be mathematically represented by:

$$PRCC(x_i, y) = \frac{\mathrm{cov}(\mathrm{rank}(x_i), \mathrm{rank}(y))}{\sigma_{\mathrm{rank}(x_i)} \sigma_{\mathrm{rank}(y)}}$$

In this formula, *cov* represents the covariance between the ranked values of x_i and y, while $\sigma_{\mathrm{rank}(x_i)}$ and $\sigma_{\mathrm{rank}(y)}$ are the standard deviations of the ranked values of x_i and y, respectively. This approach effectively captures the monotonic relationship between the variables, providing a clear measure of how changes in one variable are associated with changes in another.

To further refine our analysis, the PRCC is adjusted for the influence of confounding variables using partial correlation techniques. This adjustment is important for models where multiple interdependent variables can mask or exaggerate the relationship between the parameter of interest and the outcome. The adjusted PRCC formula is enhanced as follows:

$$PRCC_{\mathrm{adjusted}}(x_i, y|\boldsymbol{Z}) = \frac{PRCC(x_i, y) - \sum_{z \in \boldsymbol{Z}} PRCC(x_i, z) \times PRCC(z, y)}{\sqrt{1 - \sum_{z \in \boldsymbol{Z}} PRCC(x_i, z)^2} \sqrt{1 - \sum_{z \in \boldsymbol{Z}} PRCC(z, y)^2}}$$

Here, Z represents a set of other parameters that might influence the relationship between x_i and y. This adjusted coefficient provides a more accurate reflection of the true impact of x_i on y, free from the distortions caused by other variables.

Following the calculation of PRCC values, the parameters are ranked based on their absolute PRCC values. Parameters exhibiting higher absolute values are deemed to have a more significant impact on the model's output, highlighting them as key drivers of model behaviour. This prioritization facilitates targeted adjustments and refinements in the model, optimizing performance and enhancing predictive accuracy.

2.3.3. Monte Carlo simulations

Monte Carlo simulations (MCS) were utilized to study the sensitivity of building performance parameters and to optimize these parameters for improved energy efficiency and occupant comfort. This method is advantageous in handling the uncertainty and variability of input parameters, providing a comprehensive exploration of potential outcomes.

The MCS approach involved generating 30,000 random samples for each input parameter based on their observed ranges using a uniform distribution. To ensure a thorough exploration of the parameter space and capture a wide array of possible scenarios, a quasi-random sequence, specifically Sobol sequence was employed [83]. Even though we have 12,000 simulations from IDA ICE, the reason for using Monte Carlo simulations was to generate additional samples.

These quasi-random samples fill in the gaps and ensure more uniform coverage of the parameter space compared to purely random samples. This approach enhances the reliability and accuracy of the sensitivity analysis and optimization results. These generated samples were then used as inputs to a pre-trained Artificial Neural Network (ANN) model, which predicted the total energy consumption for each set of parameters. The ANN model had been previously trained on a comprehensive dataset from IDA ICE, which included 12,000 simulations.

In addition, we implemented an optimization process using MCS aimed to identify the parameter set that minimized energy consumption. The optimal set was determined by locating the sample that resulted in the minimum predicted energy consumption. This optimal parameter set was then inverse transformed to reflect the original scale of the parameters. For example, optimal settings for parameters such as room depth, U-value, and shading factor were identified, providing specific conditions under which energy efficiency is maximized.

For generating quasi-random samples using Sobol sequences, the formula can be expressed as:

$$Xi = Q(i)$$

Where Xi represents the i −th sample vector, and $Q(i)$ represents the i −th point in the Sobol sequence.

The ANN model predicts the total energy consumption based on input parameters. The prediction formula can be expressed as:

$$E = f(X)$$

where E represents the predicted energy consumption, X represents the vector of input parameters, and f represents the ANN model's function mapping input parameters to the predicted energy consumption.

Sensitivity analysis involves understanding how changes in input parameters X affect the output E using the partial derivative of the output with respect to an input parameter:

$$S_{X_j} = \frac{\partial E}{\partial X_j}$$

where S_{X_j} represents the sensitivity of the energy consumption to the j-th parameter X_j.

The goal of the optimization process is to minimize the energy consumption E by finding the optimal set of parameters X^* :

$$X^* = argminXf(X)$$

where X^* represents the optimal parameter set, and *argmin* denotes the argument of the minimum, i.e., the parameter set X those results in the minimum predicted energy consumption.

After finding the optimal parameter set in the normalized or transformed space, it is necessary to inverse transform these values back to their original scale:

$$X_{\mathrm{original}} = T^{-1}(X_{\mathrm{normalized}})$$

where X_{original} represents the parameters in their original scale, T^{-1} represents the inverse transformation function, and $X_{\mathrm{normalized}}$ represents the normalized or transformed parameters.

2.3.4. Analysis of variance (ANOVA)

In our methodology, ANOVA were also employed to evaluate the significance of individual features in our predictive models [60]. ANOVA is a statistical method used to determine the extent to which different groups vary or differ from each other, making it particularly useful for assessing feature importance in the context of model outputs. This technique helped to identify which variables significantly affect the response variable, thereby contributing to a more informed feature selection process.

The process began by fitting a linear model that incorporates all potential predictors as independent variables influencing the model's output. We then computed the ANOVA for this fitted model, which partitions the total variability observed in the model's predictions into components attributable to each feature. We were able to quantify the contribution of each feature to the model's performance by analyzing these components. Features that demonstrated a statistically significant variance in the ANOVA were considered important for affecting the model's output.

The F-value in ANOVA [84] is calculated using the ratio of the mean square between groups (MSB) to the mean square within groups (MSW):

$$F = \frac{MSB}{MSW}$$

where:

$$MSB = \frac{SSB}{df_B}$$

$$MSW = \frac{SSW}{df_W}$$

In these formulas, SSB is the sum of squares between groups, df_B is the degrees of freedom between groups, calculated as k − 1, where k is the

number of groups, *SSW* is the sum of squares within groups and df_W is the degrees of freedom within groups, calculated as N − kN, where N is the total number of observations.

The sum of squares between groups (SSB) is calculated as:

$$SSB = \sum_{i=1}^{k} n_i(\overline{Y_i} - \overline{Y})^2$$

where n_i is the number of observations in group i, $\overline{Y_i}$ is the mean of group i, and $\overline{Y}$ is the overall mean of all observations.

The sum of squares within groups (SSW) is calculated as:

$$SSW = \sum_{i=1}^{k} \sum_{j=1}^{n_i} (Y_{ij} - \overline{Y_i})^2$$

Where Y_{ij} is the j-th observation in group i.

The p-value [84] is derived from the F-distribution, considering the F-value and the degrees of freedom for both the numerator (between groups) and the denominator (within groups):

$$p = P(F_{df_B, df_W} \geq F)$$

Features exhibiting statistically significant variance in the ANOVA were considered crucial for impacting the model's output. This quantitative assessment not only facilitated the identification of features with the most substantial statistical significance but also ensured that our model remained both interpretable and computationally efficient. By prioritizing these influential features, we enhanced the model's simplicity and performance, ultimately leading to more reliable and robust predictions.

2.4. Financial assessment of Energy-Efficient HVAC solutions

In this work, a scenario-based approach integrated with a detailed financial assessment is employed to identify the most cost-effective energy-saving solutions for HVAC systems. The focus is on evaluating their long-term economic benefits under realistic operational conditions, particularly comparing various systems including Baseline HVAC, BMS (Building Management System) HVAC [85], Air-to-Water (A2W) [86], and Ground Source Heat Pump (GSHP) [87] systems.

The economic analysis begins by calculating the present value (PV) [88] of all anticipated costs over a 40-year calculation period. These costs include initial investment expenses such as purchase price, installation, and infrastructure modifications, as well as ongoing expenses like annual maintenance and energy consumption costs. Replacement costs are also considered for components with shorter lifespans than the overall calculation period. To account for the time value of money, the present value of these costs is calculated using a discounting formula, ensuring that future expenses are adjusted to their current value. The formula used is:

$$PV = \sum_{t=1}^{T} \frac{C_t}{(1+r)^t}$$

Where *PV* represents the present value, C_t is the cost at time *t*, *r* is the discount rate, and *t* is the time horizon (40 years). This calculation automated using Python's NumPy [89] and Pandas [90] libraries. These scripts handle large datasets and apply financial formulas to dynamically adjust for various economic conditions. This automation allows for real-time updates to the financial model, enabling efficient reassessment under changing conditions such as energy price fluctuations, inflation, or maintenance schedules.

To ensure accuracy in cost estimation, data is sourced from Norwegian price book [61] and NS-EN 15459–1:2017 [62]. These resources provide up-to-date information on initial investment and replacement costs, ensuring the financial analysis reflects current market conditions. Energy consumption, a key ongoing cost, is calculated based on projected annual use and anticipated electricity prices, with historical data used to inform future price forecasts. Maintenance costs, another recurring expense, are similarly modelled based on expected maintenance intervals and cost per visit [91]. To account for equipment with limited lifespans, the annualized durability cost is calculated using the formula:

$$\text{Annualized Durability Cost} = \frac{\text{Initial Cost}}{\text{Expected Lifespan (years)}}$$

Given the inherent uncertainty in future energy prices, inflation, and system performance, Monte Carlo simulations are utilized to provide a robust analysis. These simulations generate multiple scenarios by varying key input parameters, such as energy prices (ranging from 1.0 to 2.0 NOK/kWh) and inflation rates (from 3 % to 5 %), allowing for a comprehensive comparison of the long-term costs of different HVAC systems. The simulations average the results to provide a more reliable comparison between the Baseline HVAC system and the more advanced BMS HVAC, A2W, and GSHP systems. This sensitivity analysis helps illustrate how economic variables can impact the total cost of ownership, particularly highlighting the cost stability and efficiency of systems like BMS HVAC.

3. 3.Results

3.1. Machine learning results

This section presents an evaluative study of different machine learning algorithms on a dataset, gauging their performance through two error metrics: MSE and R-squared (R^2). The assessment includes a variety of models from simple linear regression to more complex architectures like the Multi-Layer Perceptron (MLP). Fig. 5 contains two bar charts comparing the performance of various machine learning models based on MSE and R-squared (R^2) scores.

In the Fig. 5, the bar charts titled "Mean Squared Error (MSE)

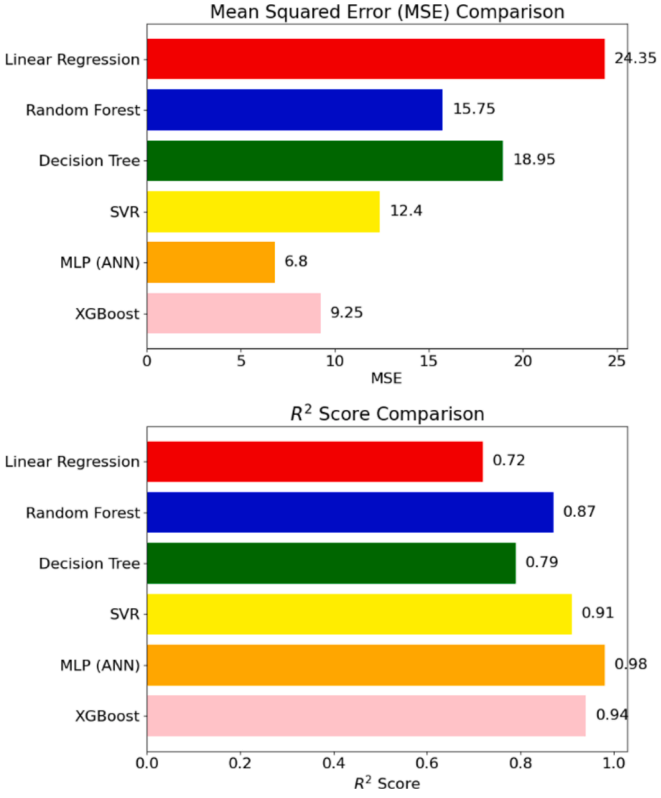

Fig. 5. Comparative Analysis of Machine Learning Models Based on MSE and R^2 Scores. The figure illustrates the performance of six different machine learning models, with the top chart displaying the MSE values and the bottom chart showing the R^2 values for each model.

Comparison," Linear Regression demonstrates the highest MSE, suggesting it has the poorest fit among the evaluated models. Random Forest and Decision Tree models exhibit moderately lower MSE values. Support Vector Regression (SVR) and Random XGBoost further reduced MSE scores, indicating better performance. The Multi-Layer Perceptron (ANN) model outperforms the others with the lowest MSE value, which implies it has the best predictive accuracy in terms of error minimization.

On the other hand, the lower bar chart, labeled "R^2 Score Comparison," the Linear Regression model again shows the least desirable outcome, with the lowest R^2 score, implying the least variance explained by the model, while MLP (ANN) has the highest scores, suggesting it has the highest proportion of variance explained, making it the most reliable model among those tested. These results imply that MLP is the superior model for this specific dataset and modeling task, with the lowest MSE and the highest R^2, indicating it is both accurate and reliable, which it has been further confirmed in Fig. 6.

3.2. One-at-a-Time (OAT) sensitivity results

Fig. 7 illustrates the OAT sensitivity analysis conducted by varying each input parameter from 50 % to 150 % of its original value, allowing for a detailed examination of the impact on total energy consumption. This range ensures that both lower and higher extremes of the parameter values are considered, providing a comprehensive understanding of their influence and allowing for the identification of optimal values and critical thresholds where the behavior of total energy consumption shifts, offering valuable insights for optimizing building design and operational strategies to enhance energy efficiency.

The OAT sensitivity analysis reveals distinct trends in how various building design and operational parameters affect total energy consumption. Notably, the room depth, U-value of the facade, and minimum air flow rate significantly influence energy use. An increase in room depth from 3 to 9 m consistently decreases energy consumption, with the lowest energy usage observed around 9 m. This reduction can be attributed to the reduced external surface area relative to the volume, minimizing heat loss or gain. Conversely, higher U-values of the facade, ranging from 0.075 to 0.225, lead to increased energy consumption, highlighting the importance of good insulation to prevent unwanted thermal exchange. The minimum air flow rate exhibits a pronounced effect, with energy consumption rising sharply as the ventilation rate increases from 0.6 to 1.8 air changes per hour. This increase underscores the significant energy demands associated with conditioning larger volumes of outdoor air.

Parameters such as the window-to-wall ratio (WWR), g-value, and reflectance exhibit non-linear relationships with energy consumption, indicating the complexity of their effects. The WWR, varying between 30 % to 90 %, shows an initial increase in energy consumption as it rises, with a relative change of up to 8 %. This suggests that larger window areas contribute to higher energy demand, likely due to greater thermal exchange. The g-value, representing the solar heat gain coefficient, exhibits a slight decrease in energy use with higher values, ranging from 0.3 to 0.6, as more solar heat is admitted, reducing heating requirements. Reflectance, varying between 0.3 and 0.9, follows a non-linear pattern, with energy consumption decreasing slightly as reflectance increases, likely due to the reduced absorption of heat and lower cooling loads.

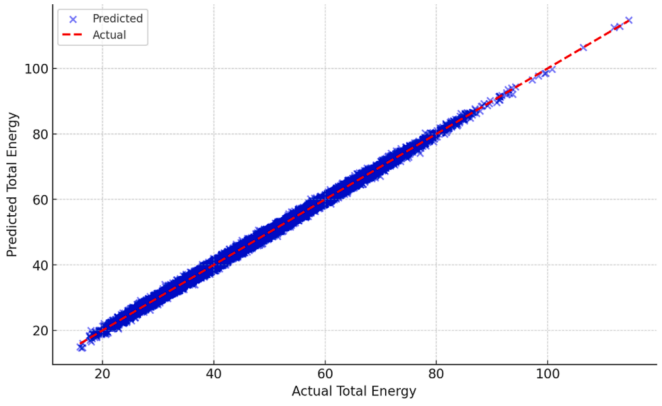

Fig. 6. The predicted versus actual total energy values. The blue crosses represent the predicted values, while the red dashed line denotes the actual values.

Operational parameters such as overhang, shading factor, and shade on consistently influence total energy consumption, although their effects are relatively moderate compared to other parameters. Increasing the overhang from 15 to 45 leads to a slight increase in energy consumption, with a relative change of about 1 %, indicating that larger overhangs may block beneficial solar gain, slightly increasing heating demands. The shading factor shows a similar trend, where increased shading from 0.4 to 0.7 leads to a modest rise in energy consumption, likely due to reduced passive solar heating and greater reliance on artificial lighting. The "shade on" parameter, varying from 40,000 to 100,000, shows a steady increase in energy demand, further emphasizing the impact of shading strategies on energy consumption.

Finally, the heat gains and lighting power density also play roles in energy consumption. Higher heat gains s, ranging from 10 to 25 W/m^2, result in slightly decreased energy consumption, likely due to internal heat gains reducing the need for external heating. Lighting power density, varying from 3 to 7 W/m^2, exhibits a slight increase in energy consumption, with a relative change of around 2 %, which might be due to the additional heat generated by lighting that needs to be countered by cooling systems.

3.3. Partial Rank correlation coefficient (PRCC) analysis results

Fig. 8 presents the outcomes of a Partial Rank Correlation Coefficient (PRCC) analysis, used to assess the strength and direction of the relationship between various input parameters and the output of a predictive model. Positive PRCC values indicate a direct correlation, while negative values suggest an inverse relationship, providing crucial insights for prioritizing factors in building performance optimization.

The PRCC analysis was undertaken to evaluate the sensitivity of energy consumption, to a range of building design and operational factors. This analysis method employs ranked data to account for potential non-linear relationships and to mitigate the influence of outliers. Each input variable was ranked, and residuals were obtained by regressing each input against all others. The output's residuals were similarly calculated by regressing the output against all input parameters. The PRCC values were then derived as the Spearman correlation coefficients between the residuals of each input parameter and the output's residuals. This method isolates the partial effect of each variable while controlling for the influence of the remaining variables.

The PRCC analysis elucidates the differential impact of various building parameters on energy consumption, vital for optimizing building designs for efficiency. The "Min air" parameter, with a PRCC value of approximately + 0.86, underscores a substantial direct influence on the model's output. This strong positive correlation likely stems from the need for greater energy to condition the increased volume of incoming air, particularly in ventilation-intensive buildings. In contrast, "Heat gains " and "Room depth" exhibit negative PRCC values of about −0.22 and −0.17, respectively. These inverse relationships suggest that higher heat gains s might lead to more efficient use of internal gains for space heating, thereby reducing the need for additional energy input. Similarly, greater room depths may enhance the passive cooling effect, particularly in deeper spaces where natural light penetration is limited and where internal areas are shaded from direct solar gains.

Additionally, parameters like "WWR" (Window-to-Wall Ratio) and

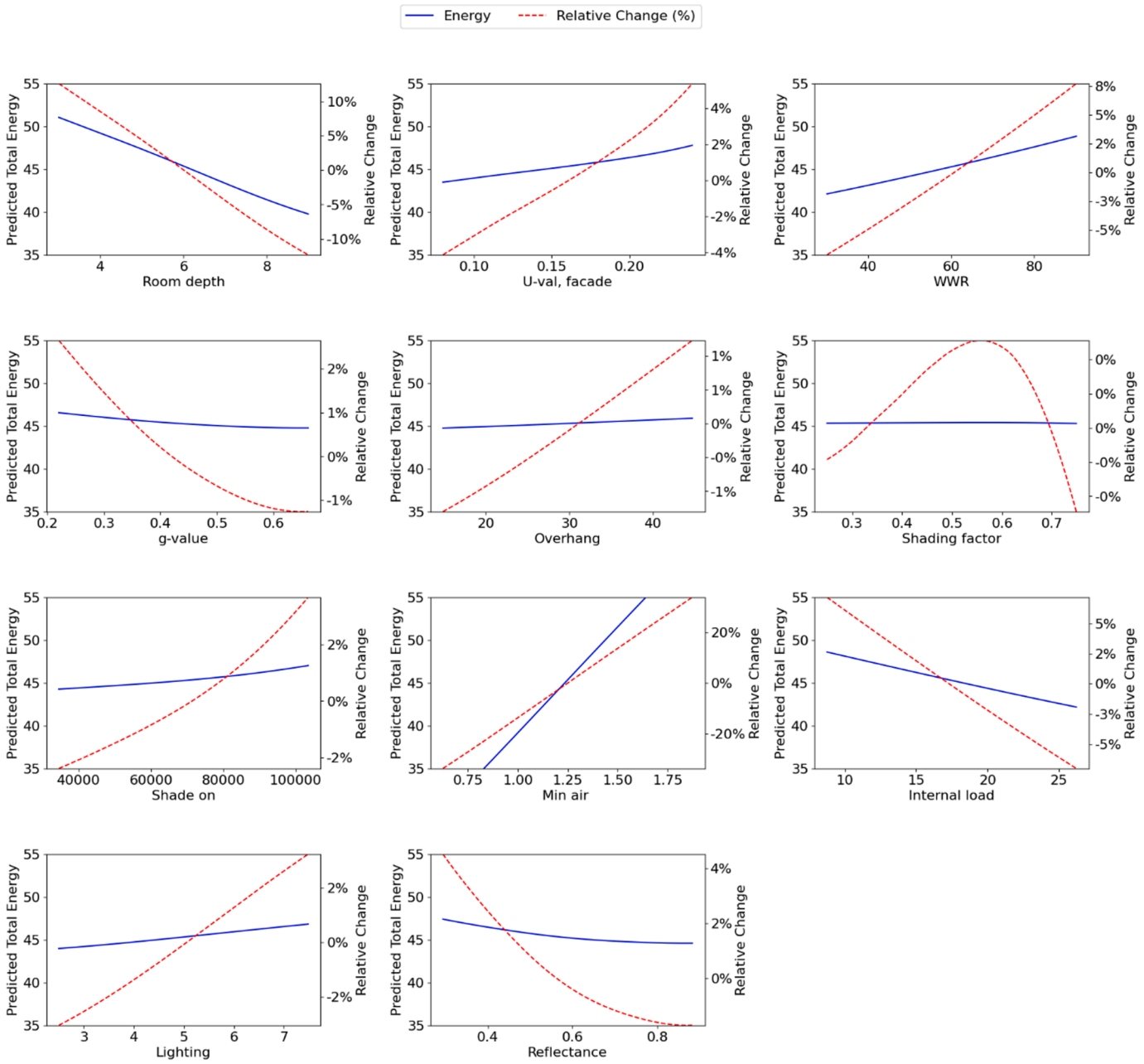

Fig. 7. Sensitivity Analysis of OAT Parametric Variations.

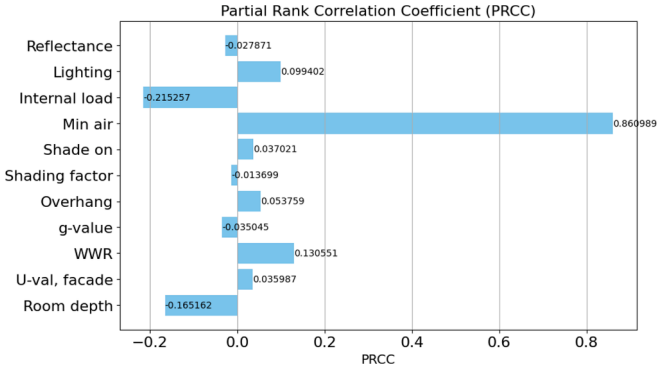

Fig. 8. PRCC Analysis of Building Design Parameters. The chart displays the Partial Rank Correlation Coefficients for various input features, indicating the strength and direction of their relationship with the model's output.

"Lighting," showing PRCC values of + 0.13 and + 0.10, respectively, indicate their significant roles. A higher WWR can increase energy requirements due to greater heat loss or gain through the windows, necessitating more energy for thermal regulation. Enhanced lighting levels correlate with increased energy consumption, not only through direct usage but also via the heat emitted by lighting fixtures, which can alter thermal loads.

3.4. Monte Carlo sensitivity results

In this analysis, the primary objective is to evaluate the sensitivity of predicted total energy consumption to variations in the input features. The process begins by loading the dataset and selecting relevant features for energy consumption analysis. These features are standardized using a StandardScaler to ensure consistency, which is important for training the neural network model, a Multilayer Perceptron Regressor (MLPRegressor) with two hidden layers (50 and 25 neurons). The model is

trained on a subset of the data, with a portion reserved for testing to ensure generalizability to unseen scenarios. To explore a wide range of possible outcomes, 1,000 random samples are generated for each feature based on their original ranges in the dataset. These samples are standardized to match the training data and fed into the trained ANN model to predict total energy consumption.

The sensitivity analysis results are visualized in Fig. 9 using scatter plots with trend lines (red for linear relations and blue for non-linear relations), highlighting the distribution of predicted energy values against randomized input values and offering insights into the variability and potential correlations within a broader range of parameter values. A key finding is the strong positive correlation observed between "Min Air" and predicted energy consumption, which is further confirmed by the PRCC analysis showing a significant positive PRCC value for "Min Air.".

The analysis also includes a detailed correlation matrix that further elaborates on these relationships in Fig. 10. For example, the matrix reveals a strong positive correlation between "Min Air" and "Predicted Energy" (0.92), underscoring the critical impact of ventilation rates on energy use. Conversely, "Heat gains " shows a moderate negative correlation (−0.22), indicating that higher heat gains s may reduce energy consumption by decreasing the need for additional heating. Other features like "Room Depth" also show a moderate negative correlation, suggesting that deeper rooms could lead to lower energy usage. Weaker positive correlations are noted for features such as "WWR" (0.2) and "Lighting" (0.16), while low correlations for "Shading Factor" and "Reflectance" suggest minimal direct impact on energy consumption.

Comparing the Monte Carlo results to the OAT sensitivity analysis, several consistent patterns emerge, although the methods reveal different aspects of parameter sensitivity. The OAT analysis showed that "Room depth" has a negative impact on energy consumption, with deeper rooms leading to lower energy use. This is corroborated by the Monte Carlo scatter plot, which shows a broad distribution but hints at lower energy values for higher room depths. Similarly, the OAT results indicated that higher U-values of the facade lead to increased energy consumption, a trend that is less clearly visible in the scatter plot due to the broader range and random sampling but still noticeable in the overall positive trend.

The g-value, which affects solar heat gain, displayed a negative correlation in both OAT and PRCC analyses. The scatter plot from the Monte Carlo analysis shows a less pronounced but still visible trend of decreasing energy consumption with increasing g-values. This consistency across methods highlights the reliability of this parameter's influence. Additionally, the "Heat gains " parameter, which showed a negative PRCC value, indicating that higher heat gains s reduce energy consumption, aligns with the scatter plot's tendency towards lower

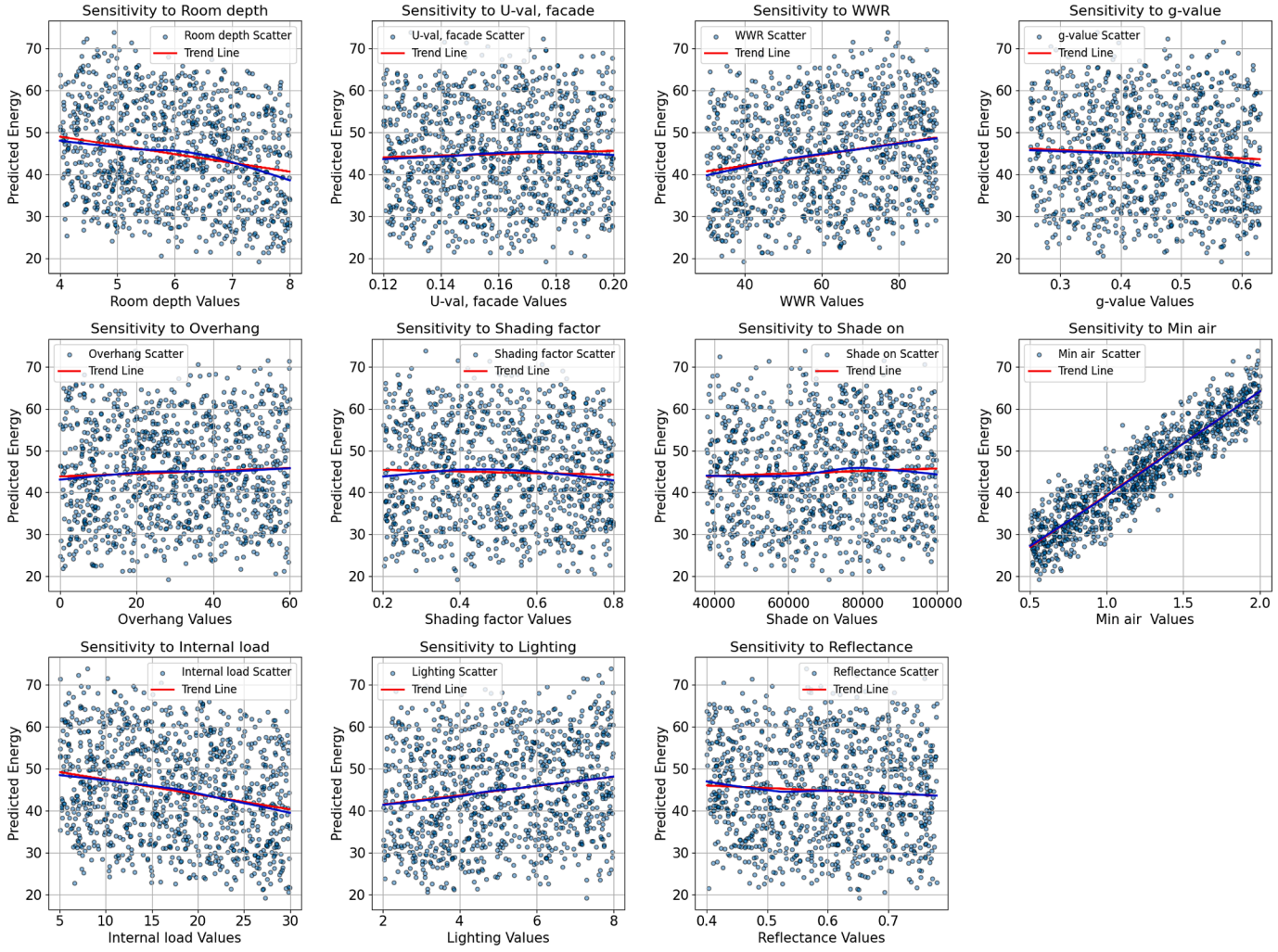

Fig. 9. Monte Carlo Sensitivity Analysis of Building Parameters. The plots display the variability in predicted output cost resulting from stochastic perturbations in building design parameters. Each subfigure shows the sensitivity of the output to changes in a specific parameter, capturing the non-linear and complex dependencies within the simulation model. These insights facilitate a probabilistic understanding of parameter impacts and support robust decision-making in building design optimization.

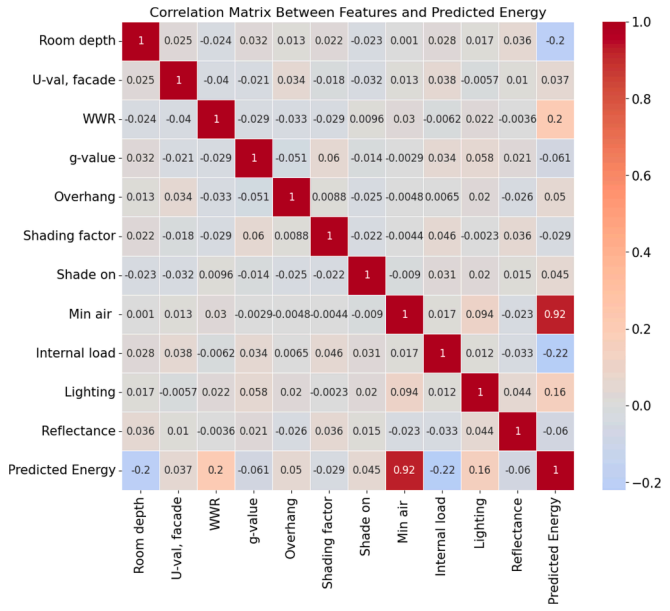

Fig. 10. Correlation Matrix Between Features and Predicted Energy Consumption. The matrix visualizes the strength and direction of relationships between input features and the predicted total energy consumption, highlighting "Min Air" as the most significant positive correlate with energy usage and "Heat gains " as a notable negative correlate.

energy values with increased heat gains s. However, the Monte Carlo analysis also reveals outliers and a wider variability that are not as apparent in the OAT analysis.

The scatter plot for "Min air" confirms the strong impact observed in both OAT and PRCC analyses. The clear positive trend indicates that increased ventilation rates result in higher energy consumption, reflecting the necessity of optimizing ventilation to balance air quality and energy efficiency. On the other hand, parameters like "Overhang" and "Shading factor," which exhibited varied and less linear impacts in OAT analysis, show a more dispersed distribution in the Monte Carlo plots, highlighting the complexity and potential non-linear effects of these parameters on energy use.

In the next step in this analysis, we extended the MCS approach by generating 30,000 samples for each input parameter within their observed ranges using a uniform distribution, ensuring a comprehensive exploration of the parameter space. These samples were then used to predict energy consumption through a pre-trained model. We identified the optimal parameter set (by optimizing multiple input parameters simultaneously) by locating the sample that resulted in the minimum predicted energy consumption. This optimal set was then inverse transformed to reflect the original scale of parameters. The distribution of predicted energies was visualized in Fig. 11, highlighting the minimum energy point, and further detailed scatter plots were employed for each parameter to investigate the sensitivity and identify the optimal points visually.

The scatter plots for room depth and U-value (façade) display a high density of prediction points across a comprehensive range of parameter values, suggesting that energy consumption remains relatively constant regardless of extensive variations in these parameters, indicating a low sensitivity to changes within the simulated conditions. The optimal points, marked in red, do not deviate significantly from the median ranges, suggesting that moderate adjustments might suffice for optimizing energy efficiency. Similarly, parameters such as window-to-wall ratio (WWR), g-value (solar gain coefficient), and overhang do not show a clear directional trend, which implies a complex and multifaceted relationship between these parameters and energy consumption. The moderate ranges of these optimal settings emphasize that extremities in parameter values are not necessarily beneficial for energy performance, highlighting the need for balanced values in effective energy management. Moreover, parameters like shading factor, demonstrates similarly complex interactions with energy consumption, as evidenced by the densely populated plots across all tested values with optimal points centered within moderate ranges. Additionally, parameters such as reflectance, minimum air change rate and heat gains also display optimal settings suggesting specific conditions under which energy efficiency is maximized.

The parameters presented in Table 6 were extracted through the MCS above where for each set, the ANN model calculated the associated energy consumption. The optimization process then identified the set of parameters that yielded the minimum energy consumption, these are the points marked in red on the scatter plots above. This optimal set represents the most energy-efficient configuration under the simulated conditions.

3.5. Analysis of variance (ANOVA) results

The ANOVA method applied in this paper is designed to statistically evaluate the influence of different building parameters on predicted energy consumption. This method segments each parameter into uniform bins (divisions of data into equal size intervals), effectively transforming continuous variables into categorical groups as can be seen in Fig. 12.

Conducting ANOVA across binned categories tests the null hypothesis [92] that all group means are equal, implying that the parameter in question does not significantly impact energy consumption. The calculation of F-values and P-values facilitates the identification of parameters that significantly differ in their effects on energy outcomes. A high F-value indicates a large variance between group means relative to the variation within groups, suggesting a strong parameter influence. Conversely, a low P-value signals that the observed variance is statistically unlikely under the null hypothesis, affirming the parameter's significant impact on energy consumption.

The ANOVA results reveal significant insights into how various building parameters affect predicted energy usage. Factors such as Room Depth, Window-to-Wall Ratio (WWR), Minimum Airflow, and Heat gains exhibit strong impacts, as evidenced by high F-values and very low P-values (e.g., Room Depth with $F = 55.3710$, $P = 4.5133e\text{-}99$, and Heat gains with $F = 85.7418$, $P = 2.9357e\text{-}154$) in Table 7. The box plots for these factors display substantial variations in predicted energy across their respective bins, underscoring their influence on energy consumption. Particularly, the Minimum Airflow factor stands out with an exceptionally high F-value of 2405.7537 and a P-value of 0.0000, indicating an extremely significant effect on energy usage, as reflected in its box plot where the trend is clear and distinct.

In contrast, other factors like the U-value of the facade, Shading Factor, and Reflectance show minimal impact on predicted energy usage, as suggested by their lower F-values and higher P-values (e.g., Shading Factor with $F = 0.5776$, $P = 8.1666e\text{-}01$, and Reflectance with $F = 0.8344$, $P = 5.8424e\text{-}01$). The box plots for these factors exhibit relatively uniform distributions across bins, implying that variations in these parameters do not lead to significant changes in energy consumption. These results suggest that modifications in U-value, Shading Factor, and Reflectance might not be effective strategies for energy efficiency improvements.

Interestingly, some factors exhibit moderate effects on energy usage. For instance, the g-value and Overhang have moderate F-values and significant P-values (e.g., g-value with $F = 3.9491$, $P = 4.8785e\text{-}05$, and Overhang with $F = 3.0245$, $P = 1.2998e\text{-}03$). The box plots for these factors show noticeable but less pronounced variations across bins, indicating their moderate influence. These factors should still be considered in energy optimization strategies, albeit with less priority compared to the more impactful factors like Minimum Airflow and Heat gains.

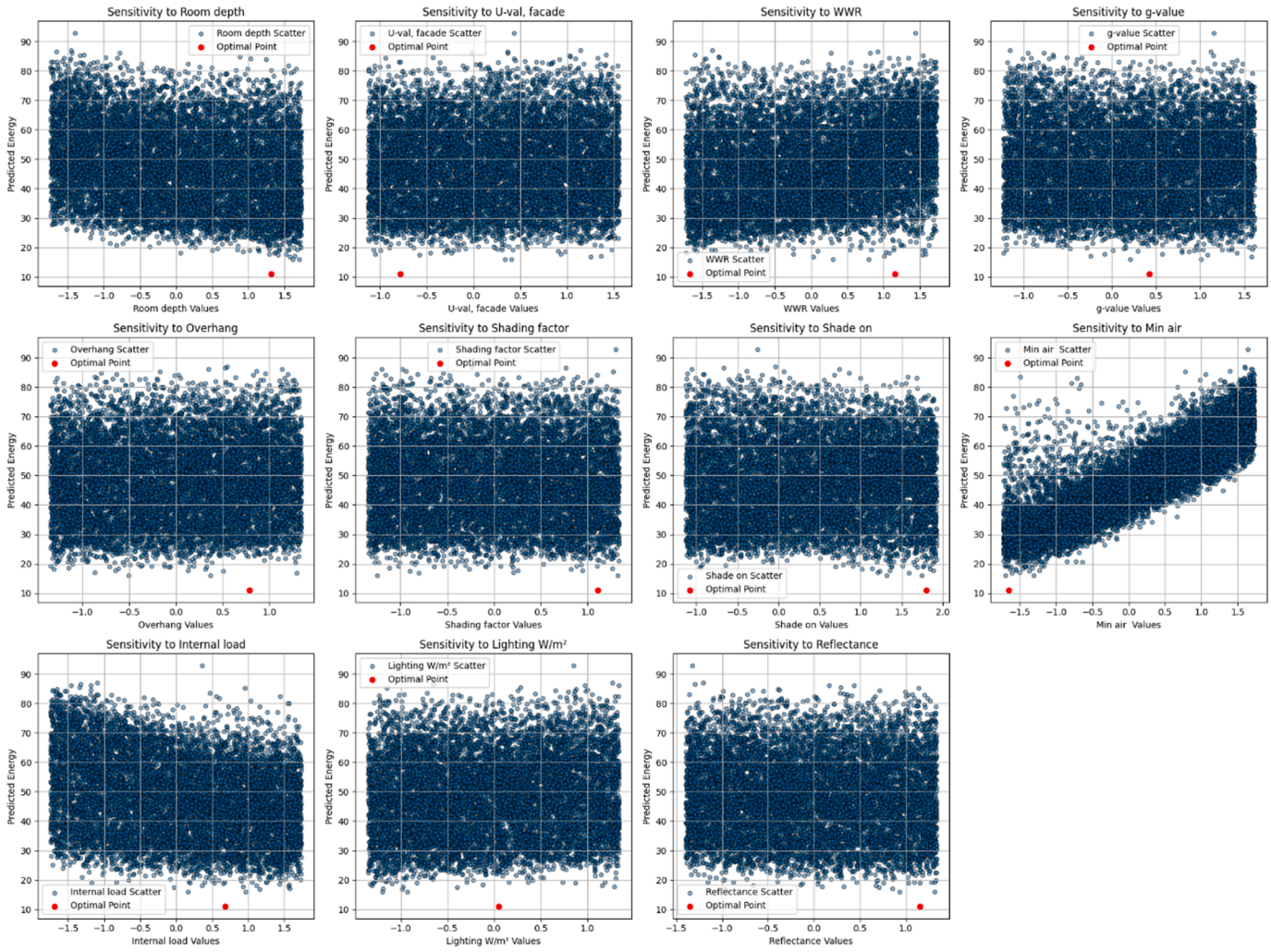

Fig. 11. The sensitivity of predicted energy consumption to various building parameters, with optimal points indicated by red dots, across a Monte Carlo simulation.

Table 6
Optimized building parameters resulting from Monte Carlo simulation, indicating the most energy-efficient settings for minimizing total energy consumption.

Parameter	Value
Room depth (m)	6.55
U-val, façade (W/(m^{2}K))	0.14
WWR (southern façade) (%)	55
g-value (−)	0.57
Overhang (cm)	40
Shading factor (−)	0.2
Shade on (lux)	38,000
Min air (ACH)	0.51
Heat gains (W/m^2)	27.63
Lighting (W/m^2)	2
Reflectance (−)	0.55
Total energy (kWh/m^2.year)	**11.05**

3.6. Thermal comfort

To identify the optimal parameters for energy efficiency and thermal comfort, we extend the ANN model with two output metrics: total energy consumption and the number of hours people experience discomfort (hours above 26 °C). The ANN architecture comprises multiple input nodes representing various building parameters and a series of hidden layers to capture complex relationships between these parameters. The outputs are the predicted total energy consumption and the number of discomfort hours, allowing for a comprehensive assessment of both energy efficiency and occupant comfort.

The structure of the ANN model is demonstrated in Fig. 13. Fig. 14 illustrates the model's accuracy in predicting the number of discomfort hours, with an R2 value of 0.98, indicating a near-perfect correlation. Similarly, the right plot shows the model's predictions for total energy consumption, achieving an R2 value of 0.95, denoting excellent predictive accuracy. These results confirm that the ANN model can reliably forecast both energy consumption and thermal comfort, facilitating the optimization of building parameters for improved energy performance and occupant well-being.

From there and through extensive simulation process using Monte Carlo, we identified specific parameter sets that achieved the best trade-offs between energy consumption and discomfort hours as seen in Fig. 15. Points closer to the lower left corner of the plot represent configurations with both low energy consumption and low discomfort hours, indicating highly efficient and comfortable building settings.

Out from this analysis, Fig. 16 present the correlation matrix illustrates the relationships between various building characteristics and their influence on thermal comfort and energy consumption. This is different from what we previously presented in the sensitive analysis, as now we are taking both energy and thermal comfort into account. Each cell represents the correlation coefficient between pairs of parameters, with values ranging from −1 to 1. Notably, WWR and g-value exhibit moderate positive correlations with the number of discomfort hours, suggesting that increases in these parameters are associated with higher

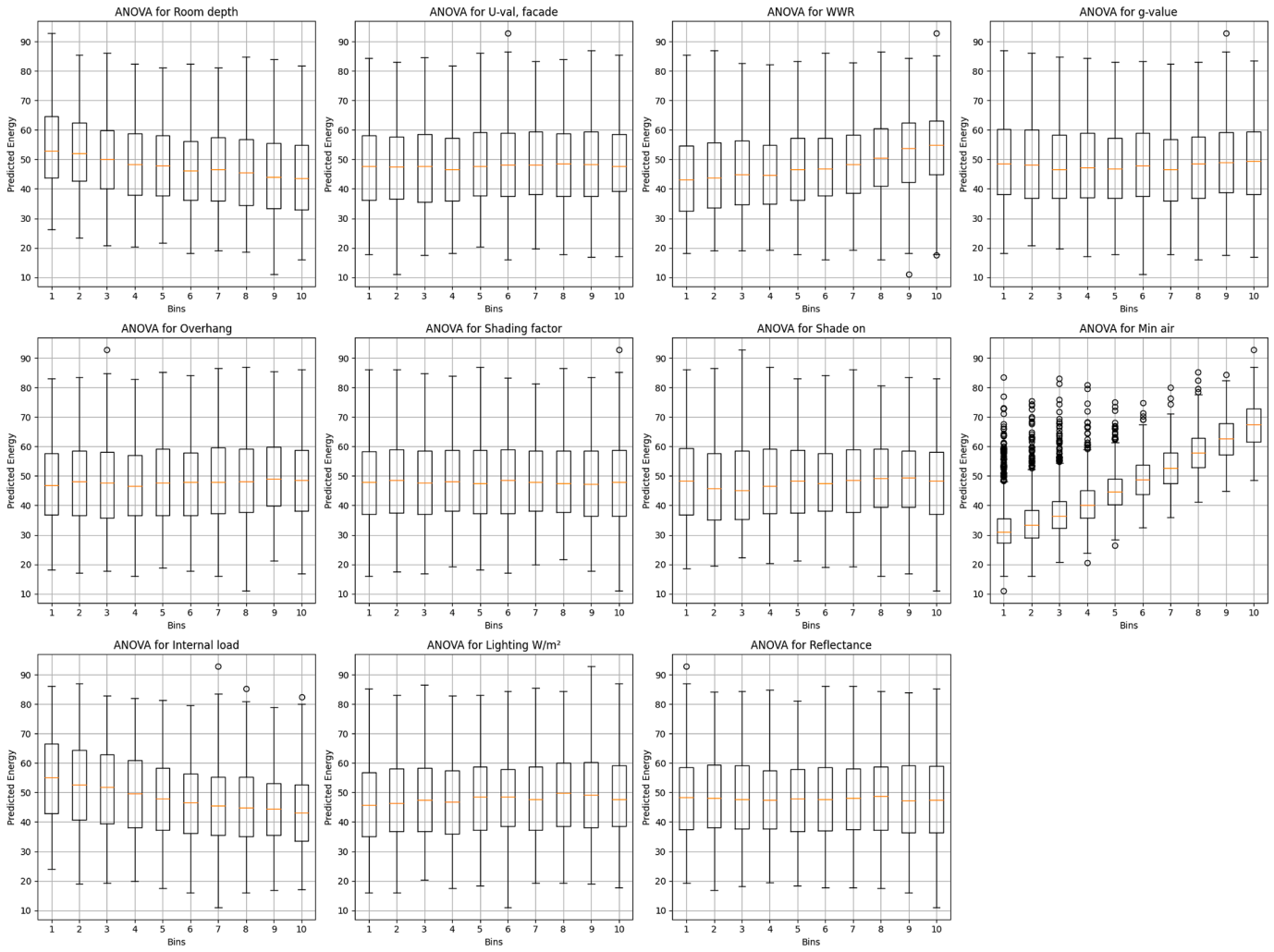

Fig. 12. The variability in predicted energy consumption across ten bins for various building parameters.

Table 7
ANOVA results showing F-values and P-values for various building parameters.

Parameter	F-value	P-value
Room depth	55.37	4.51E-99
U-val, facade	2.61	0.0050563
WWR	55.38	4.34E-99
g-value	3.94	4.88E-05
Overhang	3.02	0.0012998
Shading factor	0.57	0.81666
Shade on	2.36	0.011579
Min air	2405.75	0
Heat gains	85.74	2.94E-154
Lighting W/m^2	6.2416	7.73E-09
Reflectance	0.8344	0.58424

thermal discomfort. Conversely, Room Depth shows a slight negative correlation with discomfort hours, indicating that deeper rooms may contribute to improved thermal comfort.

Table 8 presents the best solutions. The identified solutions include a range of configurations, such as a room depth between 5.16 and 7.95 m, U-values (facade) from 0.12 to 0.20 W/(m^{2}K), and window-to-wall ratios (WWR) spanning 33 to 69 %. Notably, the shading factor varies from 0.4 to 0.8, and heat gains s range from 8.87 to 27.32 W/m^2. These configurations achieve total energy consumption between 17.39 and 22.51 kWh/m^2, with discomfort hours consistently at zero. This indicates that balanced adjustments across multiple parameters can effectively optimize both energy efficiency and thermal comfort in building design.

3.7. Economically viable energy-saving solutions

To identify the most economically viable energy-saving solutions, we have integrated scenario-based analysis with a comprehensive financial review, focusing on the HVAC system. This approach is informed by the sensitivity analyses discussed earlier in this study, which highlighted the significant impact of HVAC systems on energy consumption. Our analysis draws on data from Norwegian price book [61] and NS-EN 15459–1:2017 [62] to reflect current economic conditions in Norway. Table 9 shows the assumptions made in this study.

Fig. 19 illustrates cost analysis comparing two different HVAC systems: 1) the Baseline HVAC system and 2) the Building Management System (BMS) HVAC [37]. In this work, the term “Baseline HVAC” refers to the standard Heating, Ventilation, and Air Conditioning system used as a reference point or starting benchmark in the cost analysis. This system represents the conventional setup without the enhanced features and controls provided by a BMS HVAC. The Baseline HVAC includes basic components necessary for heating, cooling, and air circulation within a building, but it lacks advanced energy management and automation capabilities that a BMS HVAC system might incorporate. The smart control system (i.e., BMS HVAC), in contrast, dynamically responds to thermal comfort, indoor air quality requirements, and occupancy levels in conditioned spaces. It includes sensors at the field level to

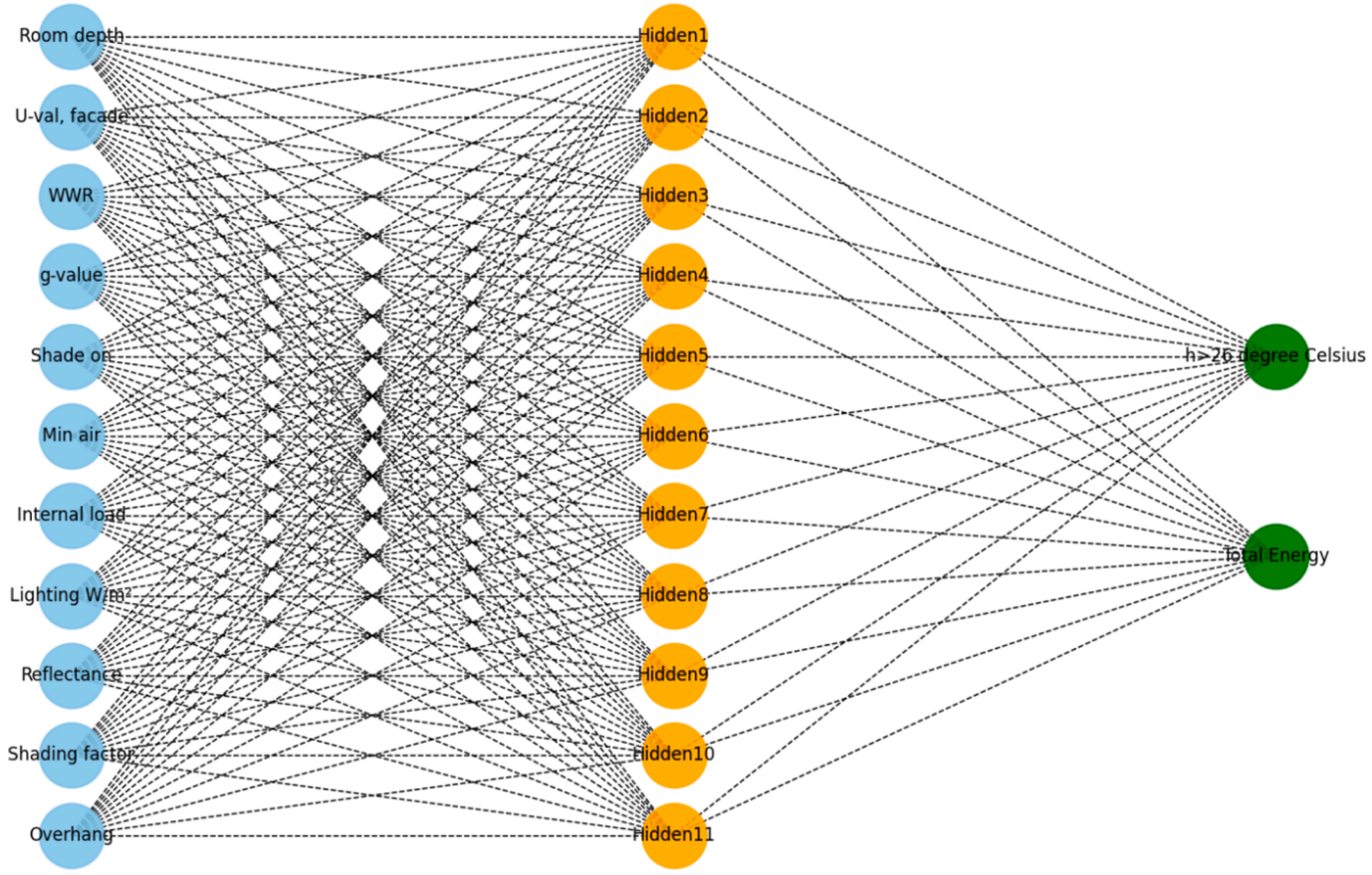

Fig. 13. The architecture of an artificial neural network (ANN) designed to predict two outputs: total energy consumption and the number of hours above 26 degrees Celsius.

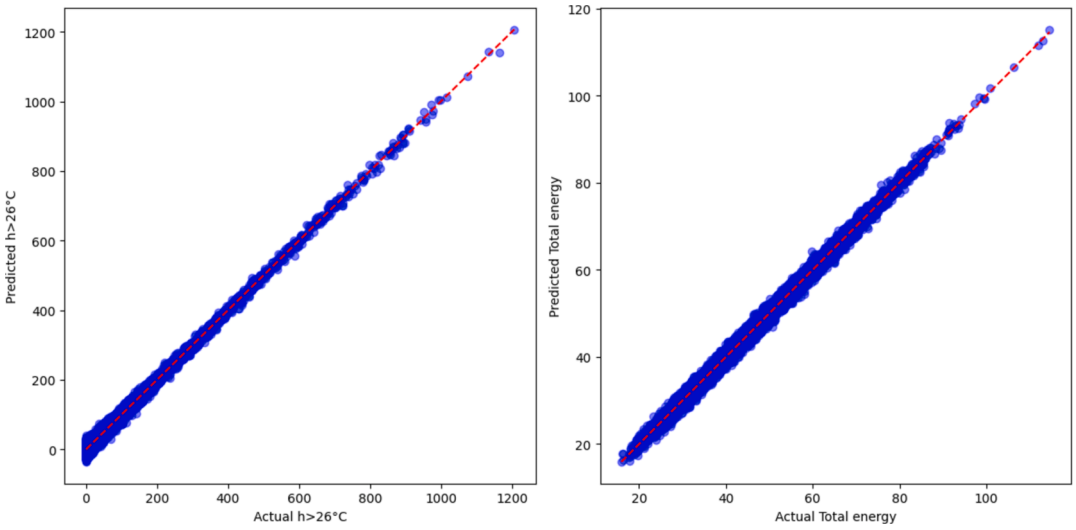

Fig. 14. Actual vs. Predicted values for discomfort hours (left) and total energy (right).

gather data on temperature, humidity, and CO_2 levels, as these are the most commonly used for HVAC applications. Occupancy sensors for lighting control are included in BMS HVAC to count occupants and the response time of HVAC systems. The smart control system employs wireless communication for data exchange among field-level devices and utilizes cloud computing for management-level tasks, chosen for their cost-effectiveness and ease of deployment, as well as their compatibility with modern IP protocols and internet usage.

In addition to the Baseline HVAC and BMS HVAC systems, two alternative systems were examined: the A2W (Air-to-Water heat pump) [94] and GSHP (Ground Source Heat Pump) [95]. Both systems were evaluated as part of the BMS HVAC setup, which increased the overall investment cost due to the integration of smart control features. These systems offer enhanced energy efficiency and leverage renewable energy sources for improved sustainability. The A2W system provides space heating and domestic hot water using a hydronic distribution method

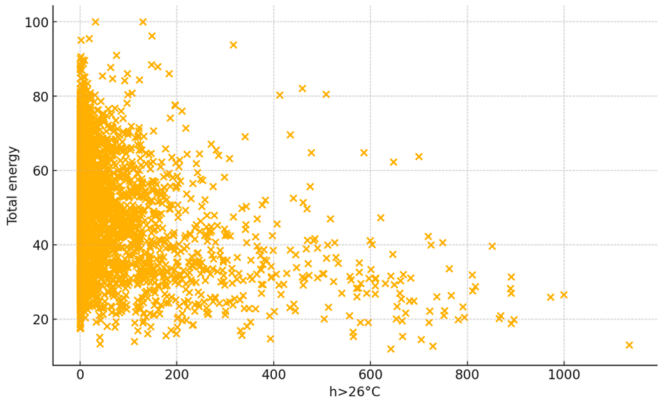

Fig. 15. Thermal comfort vs. Energy consumption.

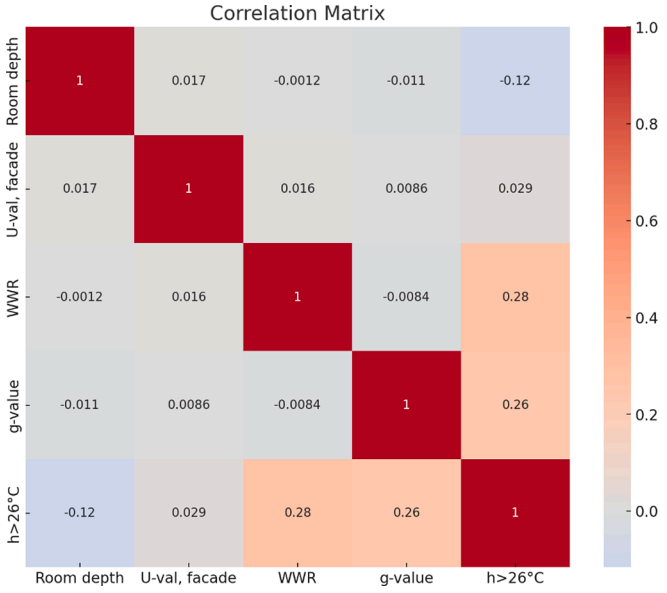

Fig. 16. Building characteristics influence on thermal comfort and energy consumption.

and incorporates a balanced ventilation system with heat recovery, reducing heating loads by preheating incoming fresh air. This system is ideal for buildings with moderate heating demands and offers a cost-effective way to lower energy consumption. The GSHP system, on the other hand, utilizes the stable temperature of the ground as a heat source, extracting geothermal energy through a borehole heat exchanger, and also features a balanced ventilation system with heat recovery. The GSHP is particularly advantageous in cold climates, where it delivers consistent heating with minimal energy usage. Both systems are equipped with auxiliary electric resistance heaters to handle peak load conditions during extreme cold periods, preventing the need for oversized systems and enhancing system longevity by reducing the frequency of on–off cycles.

This analysis breaks down the total costs into investment and operational expenses, both measured in NOK/m^2 and USD/m^2. To quantify the life cycle costs of traditional and smart control systems, we first define their characteristics, including control effectuation and the requirements and deployment of hardware. The traditional control system is characterized by a fixed, pre-programmed time-of-day operating schedule. It involves field-level devices like sensors and actuators communicating with zone controllers at the automation level, which in turn communicate with operator workstations at the management level. The system uses a wired network backbone for communication across its hierarchy, and basic thermostats in conditioned rooms provide simple functions such as ON/OFF, temperature, and fan speed selection.

To determine the costs associated with cloud computing services, an analysis of network traffic is necessary (Fig. 17). Direct measurement of traffic flows in real-life systems is often limited, so researchers frequently use testbed experiments, simulations, and external traces, although these may not fully replicate real system behavior. This study estimates traffic flow based on the supervisory control and data acquisition (SCADA) [96], noting that SCADA networks typically have stable, non-self-similar flows including diurnal trends [97]. Assuming periodic data acquisition through polling mechanisms at fixed intervals, this study estimates data generation and transfer by each device. These estimates allow for the calculation of costs related to the cloud-based smart control system, considering average network packet sizes and durations per poll to aggregate data at the control system level. For example, each device generates 500 MB of data per day with polling every 10 min, producing 144 KB of data per day per device, resulting in 14.4 MB for 100 devices daily. This translates to a monthly data generation of 432 MB, costing approximately $0.0432, given a service provider rate of $0.10 per GB.

To obtain the total cost results, a systematic approach was employed, starting with data collection. This involved gathering detailed cost data for both the Baseline and BMS HVAC systems. For the initial investment

Table 9
Economic performance evaluation details.

Parameter	Details
Costs Calculation	Present value of initial investment costs, annual maintenance costs, and energy costs over the calculation period
Replacement Costs	Replacement costs added if equipment has shorter lifetime than calculation period
Electricity Prices Historical	Average Norwegian price was 1.0 NOK/kWh from 2012 to 2020
Calculation period [years]	40
Inflation rate [%]	4
Electricity price for baseline case [NOK/kWh] [93]	1.375

Table 8
Best solutions identified through the Monte-Carlo simulation.

Room depth	U-val, facade	WWR	g-value	Overhang	Shading factor	Shade on	Min air	Heat gains	Lighting W/m^2	Reflectance	h > 26 °C	Total energy
6.62	0.12	35	0.50	0	0.4	70,000	0.52	8.87	4	0.78	0	17.39
5.30	0.18	48	0.50	60	0.8	70,000	0.77	13.89	2	0.40	0	17.82
7.35	0.14	64	0.32	60	0.4	52,000	0.54	14.71	2	0.40	0	18.44
5.79	0.14	42	0.32	20	0.8	45,000	0.55	27.32	6	0.40	0	19.42
5.16	0.12	33	0.37	60	0.4	100,000	0.54	10.44	6	0.78	0	20.10
5.62	0.18	35	0.50	20	0.8	45,000	0.69	23.99	2	0.65	0	20.55
7.23	0.12	35	0.63	0	0.6	61,000	0.71	20.60	6	0.65	0	21.23
7.21	0.20	45	0.63	40	0.8	61,000	0.51	11.30	2	0.40	0	22.10
6.57	0.14	34	0.43	20	0.4	61,000	0.94	19.27	2	0.55	0	22.44
7.95	0.20	69	0.25	60	0.8	61,000	0.64	18.97	8	0.65	0	22.51

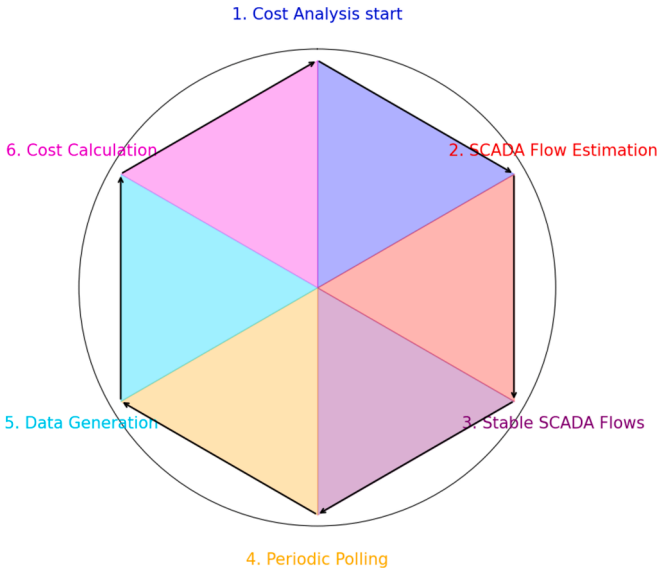

Fig. 17. Key concepts in cloud computing cost analysis framework.

costs, data included the purchase price of HVAC equipment, installation expenses, and any necessary infrastructure modifications. This data was sourced from vendor quotes, industry reports, and historical records of the case study. Furthermore, the operational costs were gathered by examining ongoing expenses such as maintenance, replacement, energy consumption, and routine servicing. Historical energy usage data was obtained from the facility's energy management system, while maintenance costs were compiled from service records and maintenance logs provided by the facility manager. These records included details on the frequency and types of maintenance activities performed on the existing HVAC system.

Next, IDA ICE was utilized to project the operational costs over a specified period by considering various factors influencing long-term costs, such as energy efficiency ratings of the HVAC systems, scheduled maintenance intervals, and the anticipated durability of the systems. For example, an HVAC system with an energy efficiency rating of 90 % operating in a building that requires 100,000 kWh annually would have an operational cost calculated based on the local energy rate, say 1 NOK per kWh, resulting in an annual energy cost of 100,000 NOK. Scheduled maintenance, estimated at 5,000 NOK per visit with four visits per year, adds another 20,000 NOK annually. Additionally, with an initial cost of 300,000 NOK and an expected lifespan of 15 years, the annualized durability cost is 20,000 NOK which was calculated as follows:

Annualized Durability Cost = Initial Cost / Expected Lifespan.

Annualized Durability Cost = 300,000 NOK / 15 years.

Annualized Durability Cost = 20,000 NOK per year.

Hence, the annualized durability cost for the HVAC system would be 20,000 NOK, which can be added to the annual operational and maintenance costs to get a more comprehensive estimate of the total annual costs.

To address the inherent uncertainties in cost estimations, Monte Carlo simulations were conducted. This involved generating iterations with varying input parameters such as fluctuating energy prices, different maintenance costs, and varying system efficiencies. The results from the Monte Carlo simulations (Fig. 18) were then averaged to facilitate a straightforward comparison between the two HVAC systems. The total costs were separated into investment and operational components, making it easier to discern the financial impact of each cost type.

The results in Fig. 19 reveal that while the BMS HVAC system may require a slightly higher initial investment compared to the Baseline HVAC system, it offers significantly lower operational costs on the long run. This suggests that the BMS HVAC system is more efficient and cost-effective over time, due to better energy management and reduced maintenance requirements. Furthermore, costs in both NOK and USD were included using a conversion rate of 1 NOK = 0.1 USD, offering a more transparent and internationally relevant representation of the results.

To further validate the findings, we consulted with facility managers. This involved a series of interviews and data-sharing sessions where we discussed the current system's performance and maintenance history.

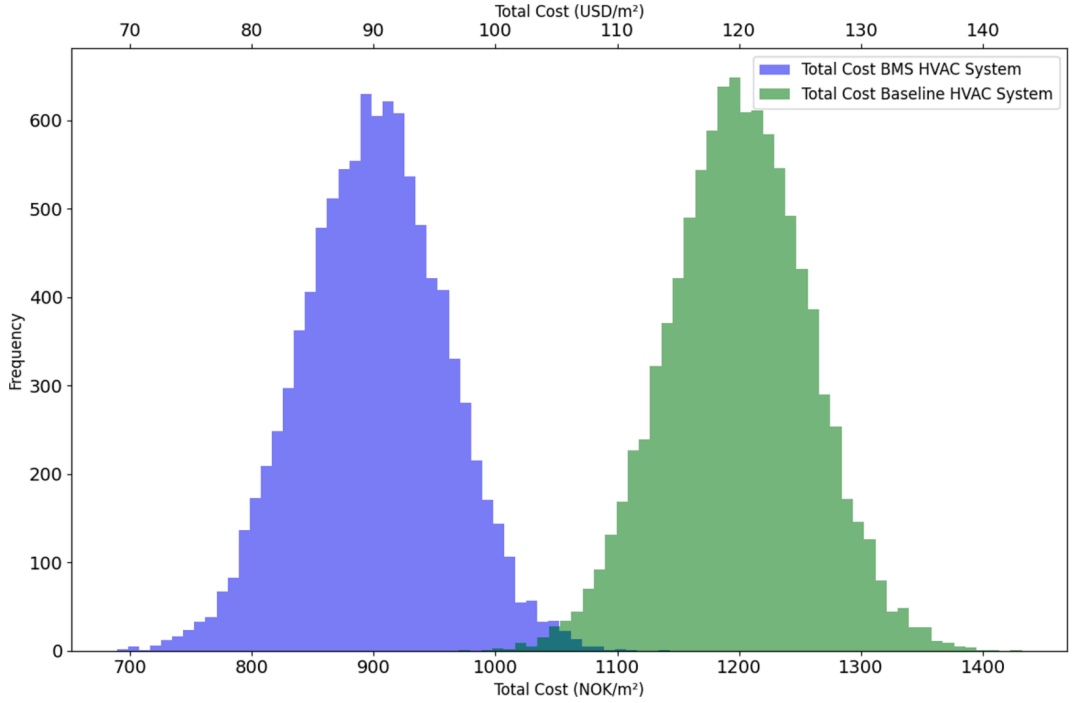

Fig. 18. Distribution of total costs for BMS and Baseline HVAC Systems (Monte Carlo Simulation).

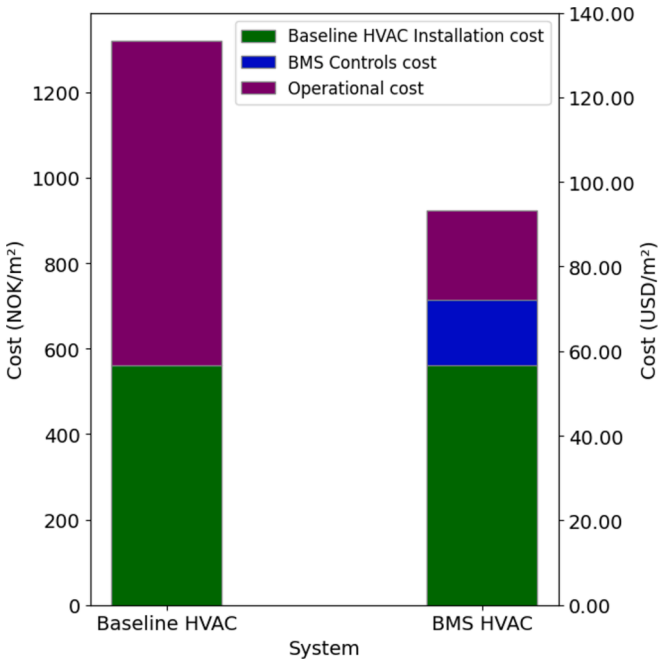

Fig. 19. Cost comparison of baseline HVAC and BMS HVAC Systems.

The facility managers provided real-world insights into practical challenges, maintenance practices, and actual energy consumption patterns observed in the facility. This collaboration ensured that the theoretical model was grounded in practical reality and reflected the actual conditions and practices of the facility.

To determine the cost differences between the Baseline HVAC and BMS HVAC systems under varying economic conditions, a comprehensive sensitivity analysis was conducted. This analysis incorporated different scenarios of inflation rates (3 %, 4 %, 5 %) and electricity prices (1.0, 1.375, 1.5, 2.0 NOK/kWh) to reflect potential future variations. Detailed cost data, including purchase price, installation expenses, maintenance costs, and energy consumption, were collected for both systems. Historical energy usage data and maintenance logs were also utilized to estimate ongoing operational expenses accurately. The analysis in Fig. 20 reveals that the Baseline HVAC system incurs significantly higher costs than the BMS HVAC system across all scenarios, with costs escalating sharply as both inflation rates and electricity prices increase. The shaded regions around the lines denote the variability in cost estimates, with the Baseline system displaying greater variability compared to the BMS system.

Furthermore, the sensitivity analysis in Fig. 21 implemented four distinct scenarios to account for varying maintenance and replacement costs. Scenario 1 considered relatively low maintenance and replacement costs for both systems. Scenario 2 increased these costs moderately, while Scenario 3 further elevated them. Scenario 4 represented the highest maintenance and replacement costs, reflecting a worst-case scenario.

Replacement activities were assumed to occur every 10 years within 40-year calculation period. Each scenario was analysed under the different inflation rates and electricity prices to evaluate their impact on the total costs of the HVAC systems. This approach provided a detailed understanding of how different economic conditions and cost assumptions affect the overall financial performance of the Baseline and BMS HVAC systems.

Consequently, several additional solutions and combinations were introduced in this study primarily focuses on the A2W and GSHP systems. The investment costs associated with these HVAC systems are shown in Fig. 22. The investment costs were carefully analysed by collecting various price points from the current Norwegian market.

To evaluate the performance of the (A2W) and GSHP systems, we calculated the *Energy Coverage Factor* (ECF) and *Seasonal Performance Factor* (SPF). The energy coverage factor is defined as the ratio between the total annual energy demand for heating and the annual heat production by the heat pump [98]. During simulations, the total heat emitted in all zones was logged along with the annual heat output of the heat pump's condenser. In scenarios where a hydronic heating system did not cover all zones, heat contributions from other emitters such as electric panel heaters and floor heating were included. The energy coverage factors calculated using IDA ICE simulations are shown in Fig. 23.

The SPF of a heat pump system is the ratio of the annual heating and cooling delivered to the building by the system to the annual electricity consumed by the system, including base and peak load heat generation. To calculate the SPF, we logged the annual heat emitted by the heat pumps' condensers and the electric boiler, along with their annual

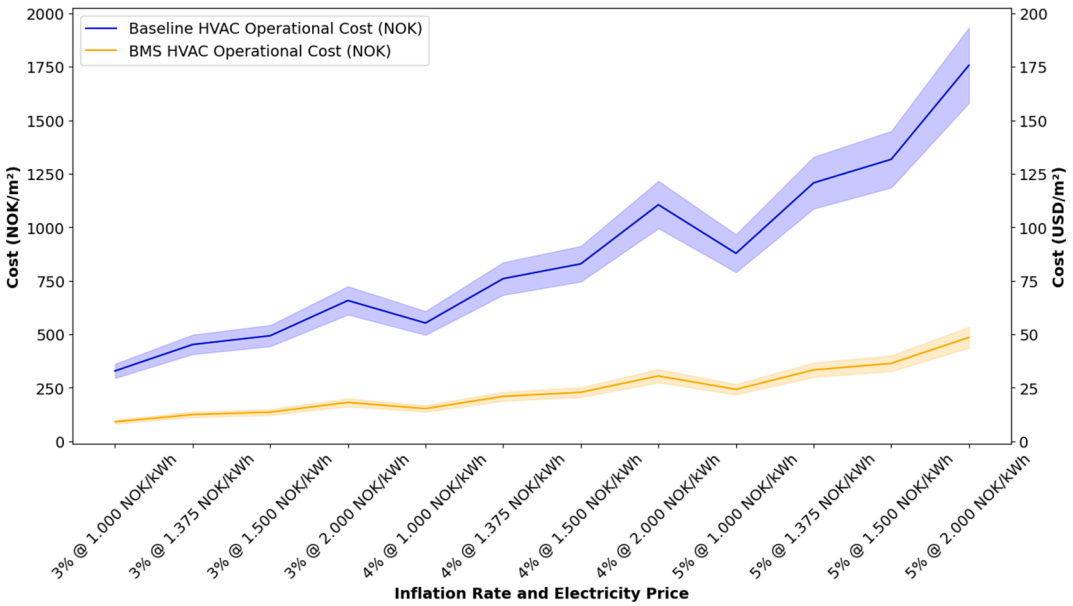

Fig. 20. Sensitivity analysis of operational costs for Baseline and BMS HVAC Systems under varying inflation rates and electricity prices.

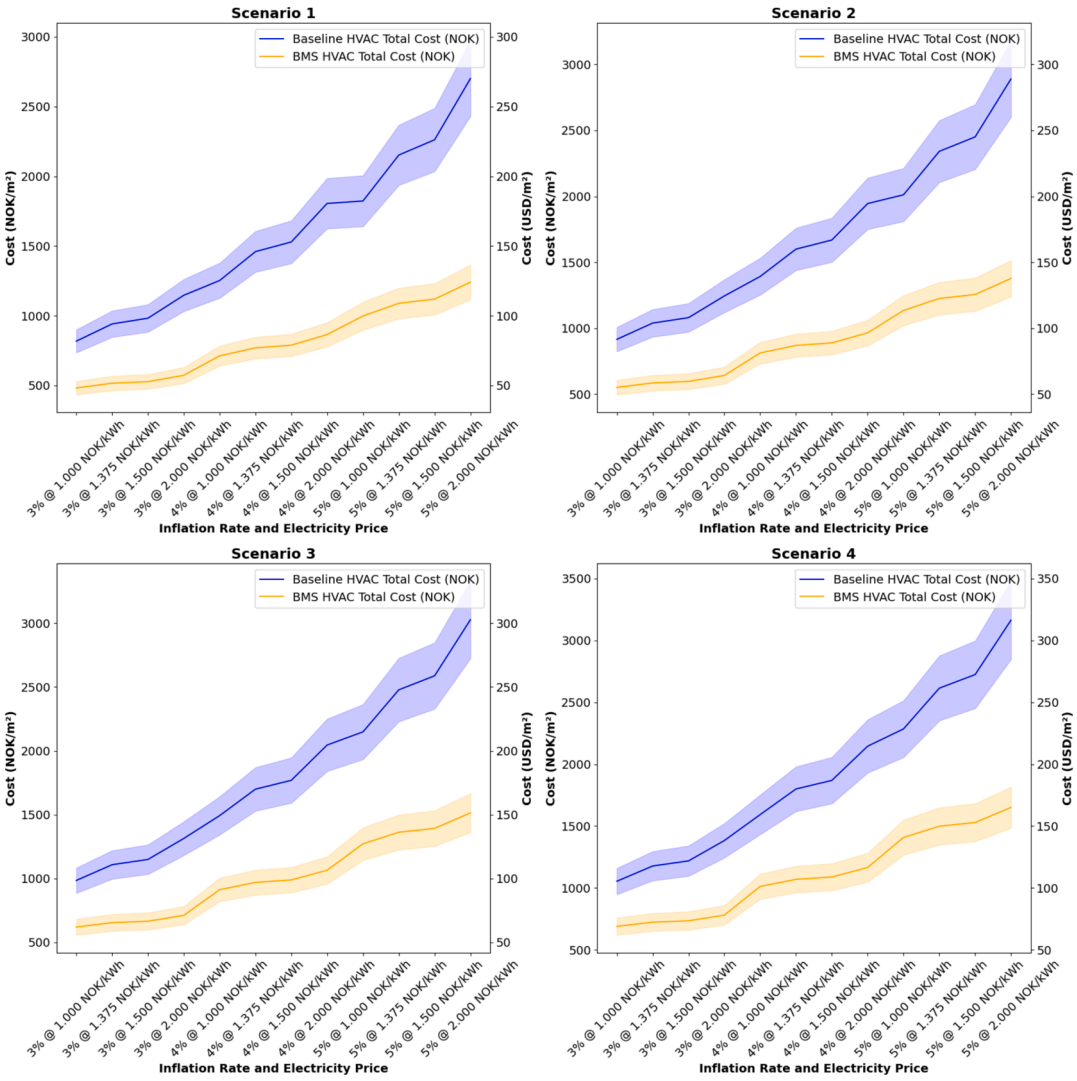

Fig. 21. Comparative analysis of Baseline and BMS HVAC System costs across four different scenarios of inflation rates and electricity prices.

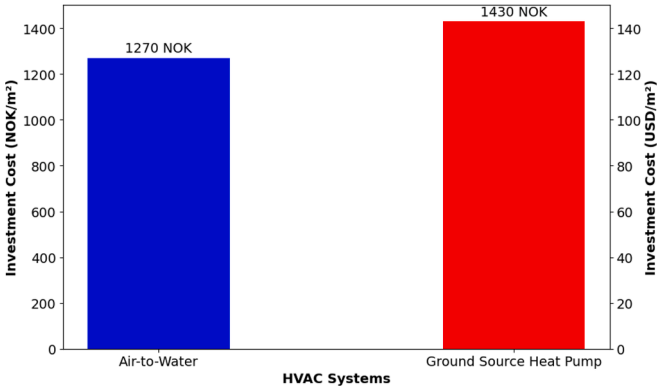

Fig. 22. Specific Investment Costs for A2W and GSHP HVAC systems (Tvedestrand).

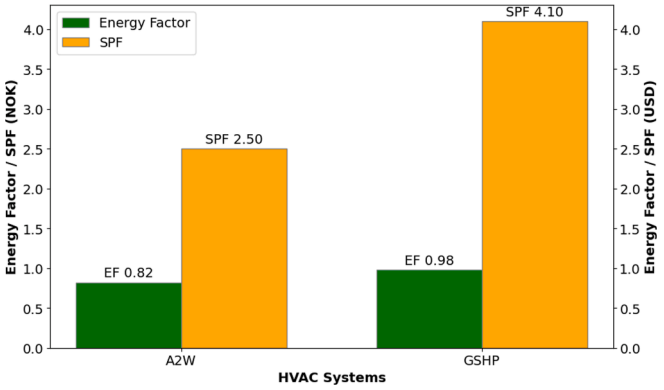

Fig. 23. Energy Coverage Factor and SPF for A2W and GSHP HVAC Combinations (Tvedestrand).

electricity consumption. The boundary conditions for SPF calculations included the heat pump, electric boiler, hydronic distribution system, and any backup direct electric space-heating system, similar to the work done in Ref. [98]. The resulting SPF values for the A2W and GSHP systems are shown in Fig. 23. The literature generally reports similar SPF values to those found in our simulations, especially in studies from cold climates such as Germany [99 100].

To assess the cost effectiveness and energy savings of various lighting systems, a detailed analysis was conducted on different lighting scenarios in IDA ICE. The analysis focused on four types of lighting systems: 1) Fluorescent Lighting, 2) LED Lighting (Standard), 3) LED Lighting (High-Efficiency), and 4) Smart LED Lighting. For each lighting type,

both the investment costs and operational costs were calculated in NOK per square meter. The energy savings were also quantified to assess the efficiency improvements offered by the more advanced lighting systems. The average electricity price of 1.375 NOK/kWh was used to standardize the cost calculations, ensuring a consistent comparison across all lighting types.

The results of the analysis were visualized in a combined bar and line chart to illustrate the investment and operational costs alongside the energy savings for each lighting system (Fig. 24). Fluorescent Lighting, representing the baseline, had the lowest investment cost but the highest operational cost and no energy savings. In contrast, Smart LED Lighting, while having the highest investment cost, showed the lowest operational cost and the highest energy savings at 12.1 %. LED Lighting (Standard) and LED Lighting (High-Efficiency) offered intermediate solutions, with progressively higher investment costs and lower operational costs, along with moderate to significant energy savings (5.4 % and 9.6 % respectively). Hence, despite the higher initial investment, advanced LED and Smart LED lighting systems provide substantial long-term operational cost savings and significant energy efficiency improvements, making them economically viable choices over time.

4. 4.Discussion

4.1. Main findings

The results of this study provide a comprehensive view of how building design parameters and operational strategies influence energy consumption and thermal comfort. Several machine learning models were evaluated for their predictive accuracy, with the MLP model emerging as the most accurate, evidenced by its lowest MSE and highest R-squared (R^2) values. This finding highlights the effectiveness of MLP in capturing the complex, nonlinear relationships between building parameters and performance outcomes.

Sensitivity analysis using various methods, OAT, PRCC, Monte Carlo simulations, and ANOVA, provided robust insights into the influence of individual parameters. The OAT analysis demonstrated that parameters such as room depth, U-value of the facade, and heat gains have significant impacts on energy consumption. Specifically, increasing room depth from 3 to 8 m consistently reduced energy use, likely due to the improved thermal mass and reduced external surface area relative to volume.

The PRCC analysis confirmed these findings, with room depth showing a negative correlation of approximately −0.10 with energy consumption, and the U-value of the facade exhibiting a positive correlation around 0.06. These results indicate that better insulation (lower U-value) and deeper rooms contribute to lower energy consumption. Monte Carlo simulations further validated these trends, demonstrating the stability and robustness of these parameters' influences across a wide range of values.

Economic impact analysis revealed that the BMS HVAC solutions offer significantly lower operational costs compared to traditional HVAC systems. This was evident from the detailed cost comparison, which showed that while the initial investment costs of BMS HVAC systems are slightly higher, the operational savings are substantial, with operational costs averaging around 150 NOK/m^2 per year. Sensitivity analyses under varying economic scenarios, including different inflation rates and electricity prices, consistently highlighted the economic viability of the BMS HVAC systems, reinforcing the long-term financial benefits of adopting advanced energy management systems.

Optimal building parameters identified in this study, such as a room depth of 6.55 m, a U-value of 0.14, a window-to-wall ratio of 55 %, and a shading factor of 0.2, achieved total energy consumption between 11.05 and 22.51 kWh/m^2 and zero discomfort hours (h > 26 °C). These recommendations provide a balanced approach to enhancing both energy efficiency and occupant comfort.

Moreover, the integration of advanced statistical and computational techniques, such as Monte Carlo simulations and ANOVA, proved essential in uncovering complex interactions between parameters. For example, the significant impact of ventilation rates on energy consumption, identified through both PRCC and Monte Carlo analyses, highlights the need for precise control of ventilation in energy-efficient building designs.

The study's approach, combining machine learning, sensitivity analysis, and economic evaluation, addresses critical gaps in existing research. It provides a strong framework for understanding the stability and robustness of optimization solutions in building performance. These findings are helpful for stakeholders, enabling informed decisions that balance technical soundness with financial viability.

4.2. Comparison with existing algorithms and sensitivity analysis techniques

Several recent studies have employed MLP and other machine learning models, often with optimization algorithms, to predict and optimize building performance. For example, Zhou et al. used a teaching–learning-based optimization (TLBO) to improve MLP's prediction accuracy, reducing error by 20 % [101]. However, while their TLBO-MLP achieved high accuracy, the computational overhead and

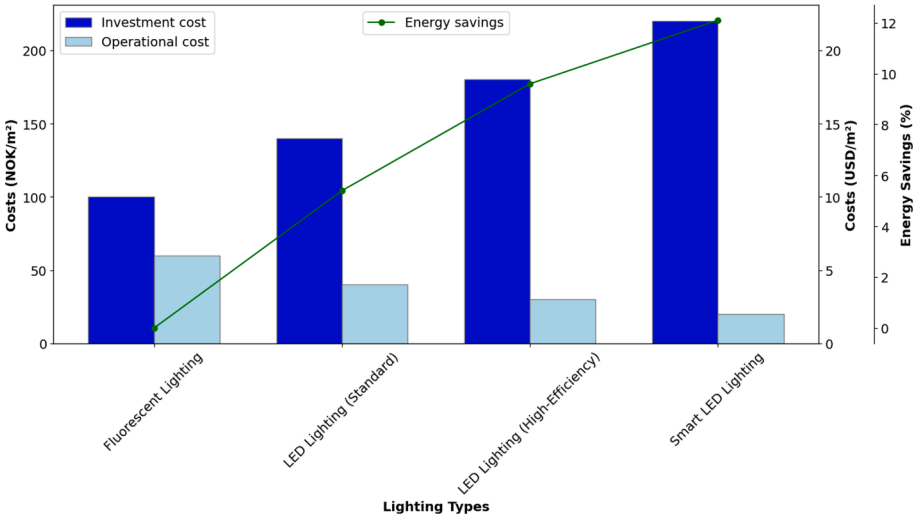

Fig. 24. Investment, Operational Costs and Energy Savings for Different Lighting Types.

complexity in training were higher compared to our streamlined approach, where sensitivity analysis combined with Monte Carlo simulations provided similar accuracy with significantly reduced computational cost. Our method avoids the need for complex optimization techniques by leveraging MCS to explore parameter uncertainties more efficiently.

Similarly, Ilbeigi et al. applied MLP with a genetic algorithm (GA) to optimize energy consumption in an office building, achieving a 35 % reduction in energy usage [102]. While this result demonstrates the effectiveness of combining MLP with optimization algorithms, their approach lacks detailed sensitivity analysis, which limits the ability to isolate the impact of individual variables. In contrast, our model integrates sensitivity analysis methods, such as PRCC and ANOVA, allowing us to pinpoint the influence of specific building parameters on energy consumption and optimize accordingly. This additional layer of analysis improves the precision and interpretability of our predictions.

Monte Carlo simulations have been extensively used to improve prediction accuracy by handling uncertainties in building performance models. Aminpour et al. demonstrated the efficacy of MCS in enhancing the computational efficiency of machine learning models by 500 times in reliability analysis [103]. While their approach focused on geotechnical reliability, our research applies MCS to building energy performance, offering similar efficiency gains with a more focused application in HVAC systems. Our combined use of MLP and MCS improves both speed and accuracy, outpacing models that do not integrate sensitivity analyses as robustly.

OAT and PRCC sensitivity analysis techniques are commonly used to assess the significance of individual parameters in energy consumption models. Kalogeras et al. applied these methods to identify influential parameters but did not combine them with machine learning [104]. In contrast, our approach integrates sensitivity analysis directly with MLP models, offering a more holistic and optimized prediction of building performance. This fusion allows for quicker identification of critical design parameters while maintaining high predictive accuracy, surpassing purely statistical or machine learning models.

ANOVA-based sensitivity analysis, as used in our study, has proven crucial for analysing the influence of multiple variables simultaneously. While Hu et al. introduced functional ANOVA for explaining machine learning models [105], our application of ANOVA with MLP is more focused on actionable insights for building performance, providing interpretability and optimized operational parameters that lead to tangible energy savings.

5. Conclusion

This study has demonstrated the significant potential of machine learning techniques to optimize building performance for energy efficiency and occupant comfort. Through a comprehensive sensitivity analysis and economic impact evaluation, critical insights into the interactions between various building design parameters have been revealed. Key findings highlight room depth, U-value of the facade, and heat gains play fundamental roles in determining energy consumption.

Additionally, the economic analysis emphasized the long-term benefits of BMS HVAC solutions, which, despite higher initial costs, offer considerable operational savings and enhanced financial viability. Also, the integration of advanced computational techniques such as Monte Carlo Simulation (MCS) and Analysis of Variance (ANOVA) has provided a robust framework for understanding the stability and reliability of optimization solutions. These methods were instrumental in identifying critical parameters and their interactions, which lays the groundwork for more effective and energy-efficient building designs.

While this study is based on the specific case of Tvedestrand Upper Secondary School in Norway, the findings offer valuable insights that are applicable to similar educational facilities in cold climates. The analysis of design parameters such as U-values, window-to-wall ratios, and heat gains s sheds light on how energy consumption can be optimized in regions where heating demands are significant. However, to enhance the generalizability of the results, future research should explore different building types, such as commercial offices, residential buildings, and mixed-use complexes, to better understand how energy performance varies across diverse settings.

Moreover, expanding the scope to include different climatic conditions across Europe would provide a broader understanding of building energy dynamics. For instance, in Mediterranean and southern European climates, where cooling loads dominate, and they are expected to dominate even more in the future, a different set of interactions between parameters such as shading devices, thermal mass, and cooling systems would likely emerge. Conducting similar analyses in warmer or more variable climates could yield new insights and enable the development of optimized, climate-adaptive design strategies that are applicable to a wide range of geographic regions. This would provide broader guidelines for building designers and engineers working in diverse contexts, making the findings of this study more widely applicable.

Future research should also incorporate real-time data from smart sensors and IoT devices to improve the accuracy of predictive models. Adaptive control systems that learn from real-time data and adjust to changing environmental conditions or occupant behaviors would be a significant advancement. These systems would enhance both performance and energy savings, contributing to more responsive and efficient building designs.

The integration of renewable energy sources, such as solar panels, wind turbines, and geothermal systems, into building energy management systems is another critical area for future exploration. Optimization algorithms could be developed to manage the interaction between renewable and traditional energy sources more effectively. In addition, a holistic life cycle assessment (LCA) that considers the environmental impacts of building materials, construction processes, and end-of-life scenarios will provide a more comprehensive view of sustainable building practices, guiding better material and design choices that minimize environmental footprints.

Finally, user-centric design approaches that incorporate occupant feedback into the optimization process will enhance both energy efficiency and occupant satisfaction. Machine learning models can be further refined to take into account user preferences and real-world feedback, ensuring that designs meet both technical and human-centered performance criteria.

CRediT authorship contribution statement

Haidar Hosamo: Writing – review & editing, Writing – original draft, Visualization, Validation, Software, Methodology, Formal analysis, Data curation, Conceptualization. **Guilherme B. A. Coelho:** Conceptualization, Formal analysis, Methodology, Writing – original draft, Writing – review & editing. **Christian Nordahl Rolfsen:** Conceptualization, Investigation, Methodology, Writing – original draft, Writing – review & editing. **Dimitrios Kraniotis:** Conceptualization, Formal analysis, Methodology, Validation, Writing – original draft, Writing – review & editing.

Declaration of competing interest

The authors declare that they have no known competing financial interests or personal relationships that could have appeared to influence the work reported in this paper.

Acknowledgments

The case study presented in this journal paper was kindly provided by Scandinavian Sustainable Circular Construction (S2C) and the University of Agder. The second author is grateful for the Foundation for Science and Technology's support through funding UIDB/04625/2020 from the research unit CERIS (DOI: 10.54499/UIDB/04625/2020).

Data availability

The authors do not have permission to share data.

References

[1] F.S. Hafez, et al., Energy Efficiency in Sustainable Buildings: A Systematic Review with Taxonomy, Challenges, Motivations, Methodological Aspects, Recommendations, and Pathways for Future Research, Energy Strategy Rev. 45 (Jan. 2023) 101013, https://doi.org/10.1016/j.esr.2022.101013.

[2] Q. Hassan, et al., The renewable energy role in the global energy Transformations, Renew. Energy Focus 48 (Mar. 2024) 100545, https://doi.org/10.1016/j.ref.2024.100545.

[3] H. Hosamo, G.B.A. Coelho, E. Buvik, S. Drissi, D. Kraniotis, Building sustainability through a novel exploration of dynamic LCA uncertainty: Overview and state of the art, Build. Environ. 264 (Oct. 2024) 111922, https://doi.org/10.1016/j.buildenv.2024.111922.

[4] H. L. Gauch, C. F. Dunant, W. Hawkins, and A. Cabrera Serrenho, "What really matters in multi-storey building design? A simultaneous sensitivity study of embodied carbon, construction cost, and operational energy," *Appl. Energy*, vol. 333, p. 120585, Mar. 2023, doi: 10.1016/j.apenergy.2022.120585.

[5] D. Kumar, M. Alam, P.X.W. Zou, J.G. Sanjayan, R.A. Memon, Comparative analysis of building insulation material properties and performance, Renew. Sustain. Energy Rev. 131 (Oct. 2020) 110038, https://doi.org/10.1016/j.rser.2020.110038.

[6] M. Norouzi, M. Chàfer, L.F. Cabeza, L. Jiménez, D. Boer, Circular economy in the building and construction sector: A scientific evolution analysis, J. Build. Eng. 44 (Dec. 2021) 102704, https://doi.org/10.1016/j.jobe.2021.102704.

[7] H.H. Hosamo, M.S. Tingstveit, H.K. Nielsen, P.R. Svennevig, K. Svidt, Multiobjective optimization of building energy consumption and thermal comfort based on integrated BIM framework with machine learning-NSGA II, Energy Build. 277 (Dec. 2022) 112479, https://doi.org/10.1016/j.enbuild.2022.112479.

[8] P. Nilsson, Achieving the Desired Indoor Climate, Studentlitteratur AB (2003).

[9] A. Yang, M. Han, Q. Zeng, Y. Sun, Adopting Building Information Modeling (BIM) for the Development of Smart Buildings: A Review of Enabling Applications and Challenges, Adv. Civ. Eng. 2021 (Mar. 2021) e8811476.

[10] F. Zhang, A.P.C. Chan, A. Darko, Z. Chen, D. Li, Integrated applications of building information modeling and artificial intelligence techniques in the AEC/FM industry, Autom. Constr. 139 (Jul. 2022) 104289, https://doi.org/10.1016/j.autcon.2022.104289.

[11] M.Q. Huang, J. Ninić, Q.B. Zhang, BIM, machine learning and computer vision techniques in underground construction: Current status and future perspectives, Tunn. Undergr. Space Technol. 108 (Feb. 2021) 103677, https://doi.org/10.1016/j.tust.2020.103677.

[12] A. Shabani, H. Hosamo, V. Plevris, and M. Kioumarsi, "A Preliminary Structural Survey of Heritage Timber Log Houses in Tonsberg, Norway," *12th Int. Conf. Struct. Anal. Hist. Constr. SAHC*, vol. Interdisciplinary projects and case studies, Nov. 2021, doi: 10.23967/sahc.2021.012.

[13] S. Zheng, T. Zeng, X. Wu, Y. Qin, W. Xu, Building Energy Consumption Control Based on BIM and Machine Learning, J. Phys. Conf. Ser. 2333 (1) (Aug. 2022) 012015, https://doi.org/10.1088/1742-6596/2333/1/012015.

[14] S. Mulero-Palencia, S. Álvarez-Díaz, and M. Andrés-Chicote, "Machine Learning for the Improvement of Deep Renovation Building Projects Using As-Built BIM Models," *Sustainability*, vol. 13, no. 12, Art. no. 12, Jan. 2021, doi: 10.3390/su13126576.

[15] S. Habibi, The promise of BIM for improving building performance, Energy Build. 153 (Oct. 2017) 525–548, https://doi.org/10.1016/j.enbuild.2017.08.009.

[16] D.K. Jung, D.H. Lee, J.H. Shin, B.H. Song, S.H. Park, Optimization of Energy Consumption Using BIM-Based Building Energy Performance Analysis, Appl. Mech. Mater. 281 (2013) 649–652, https://doi.org/10.4028/www.scientific.net/AMM.281.649.

[17] C. Fan, F. Xiao, C. Yan, C. Liu, Z. Li, J. Wang, A novel methodology to explain and evaluate data-driven building energy performance models based on interpretable machine learning, Appl. Energy 235 (Feb. 2019) 1551–1560, https://doi.org/10.1016/j.apenergy.2018.11.081.

[18] M. B. Mohammad Rahmani Asl, "BIM-based Parametric Building Energy Performance Multi-Objective Optimization," in *Thompson, Emine Mine (ed.), Fusion - Proceedings of the 32nd eCAADe Conference - Volume 2, Department of Architecture and Built Environment, Faculty of Engineering and Environment, Newcastle upon Tyne, England, UK, 10-12 September 2014, pp. 455-464*, CUMINCAD, 2014. Accessed: Apr. 12, 2024. [Online]. Available: https://papers.cumincad.org/cgi-bin/works/paper/ecaade2014_224.

[19] D. Zhuang, et al., A performance data integrated BIM framework for building life-cycle energy efficiency and environmental optimization design, Autom. Constr. 127 (Jul. 2021) 103712, https://doi.org/10.1016/j.autcon.2021.103712.

[20] M. Rätz, A.P. Javadi, M. Baranski, K. Finkbeiner, D. Müller, Automated data-driven modeling of building energy systems via machine learning algorithms, Energy Build. 202 (Nov. 2019) 109384, https://doi.org/10.1016/j.enbuild.2019.109384.

[21] C. van Treeck, R. Wimmer, T. Maile, BIM for Energy Analysis, in: A. Borrmann, M. König, C. Koch, J. Beetz (Eds.), Building Information Modeling: Technology Foundations and Industry Practice, Springer International Publishing, Cham, 2018, pp. 337–347, https://doi.org/10.1007/978-3-319-92862-3_20.

[22] L. Zhao, W. Zhang, and W. Wang, "BIM-Based Multi-Objective Optimization of Low-Carbon and Energy-Saving Buildings," *Sustainability*, vol. 14, no. 20, Art. no. 20, Jan. 2022, doi: 10.3390/su142013064.

[23] S. Järvistö, "Renovation strategies for the energy consumption of a 1954 single-family house using IDA-ICE." Accessed: Sep. 29, 2024. [Online]. Available: http://www.theseus.fi/handle/10024/804197.

[24] M. Rabani, H. Bayera Madessa, and N. Nord, "Achieving zero-energy building performance with thermal and visual comfort enhancement through optimization of fenestration, envelope, shading device, and energy supply system," *Sustain. Energy Technol. Assess.*, vol. 44, p. 101020, Apr. 2021, doi: 10.1016/j.seta.2021.101020.

[25] D. Mazzeo, N. Matera, C. Cornaro, G. Oliveti, P. Romagnoni, L. De Santoli, EnergyPlus, IDA ICE and TRNSYS predictive simulation accuracy for building thermal behaviour evaluation by using an experimental campaign in solar test boxes with and without a PCM module, Energy Build. 212 (Apr. 2020) 109812, https://doi.org/10.1016/j.enbuild.2020.109812.

[26] C.J. Hopfe, R.S. McLeod, Enhancing resilient community decision-making using building performance simulation, Build. Environ. 188 (Jan. 2021) 107398, https://doi.org/10.1016/j.buildenv.2020.107398.

[27] S. Yip, A.K. Athienitis, B. Lee, Early stage design for an institutional net zero energy archetype building. Part 1: Methodology, form and sensitivity analysis, Sol. Energy 224 (Aug. 2021) 516–530, https://doi.org/10.1016/j.solener.2021.05.091.

[28] S. Attia, "Computational Optimisation for Zero Energy Building Design, Interviews with Twenty Eight International Experts," 2012, Accessed: Apr. 16, 2024. [Online]. Available: https://orbi.uliege.be/handle/2268/168345.

[29] S. Attia, M. Hamdy, W. O'Brien, S. Carlucci, Assessing gaps and needs for integrating building performance optimization tools in net zero energy buildings design, Energy Build. 60 (May 2013) 110–124, https://doi.org/10.1016/j.enbuild.2013.01.016.

[30] T. Østergård, R.L. Jensen, S.E. Maagaard, Building simulations supporting decision making in early design – A review, Renew. Sustain. Energy Rev. 61 (Aug. 2016) 187–201, https://doi.org/10.1016/j.rser.2016.03.045.

[31] N.D. Lagaros, V. Plevris, N. Ath, Kallioras, "The Mosaic of Metaheuristic Algorithms in Structural Optimization", Arch. Comput. Methods Eng. 29 (7) (Nov. 2022) 5457–5492, https://doi.org/10.1007/s11831-022-09773-0.

[32] V. Plevris and G. Solorzano, "A Collection of 30 Multidimensional Functions for Global Optimization Benchmarking," *Data*, vol. 7, no. 4, Art. no. 4, Apr. 2022, doi: 10.3390/data7040046.

[33] E. Marsh, S. Allen, L. Hattam, Tackling uncertainty in life cycle assessments for the built environment: A review, Build. Environ. 231 (Mar. 2023) 109941, https://doi.org/10.1016/j.buildenv.2022.109941.

[34] S. mohammad E. Saryazdi, A. Etemad, A. Shafaat, and A. M. Bahman, "A comprehensive review and sensitivity analysis of the factors affecting the performance of buildings equipped with Variable Refrigerant Flow system in Middle East climates," *Renew. Sustain. Energy Rev.*, vol. 191, p. 114131, Mar. 2024, doi: 10.1016/j.rser.2023.114131.

[35] S. Imam, D.A. Coley, I. Walker, The building performance gap: Are modellers literate? Build. Serv. Eng. Res. Technol. 38 (3) (May 2017) 351–375, https://doi.org/10.1177/0143624416684641.

[36] H.H. Hosamo, H.K. Nielsen, D. Kraniotis, P.R. Svennevig, K. Svidt, Digital Twin framework for automated fault source detection and prediction for comfort performance evaluation of existing non-residential Norwegian buildings, Energy Build. 281 (Feb. 2023) 112732, https://doi.org/10.1016/j.enbuild.2022.112732.

[37] H.H. Hosamo, H.K. Nielsen, D. Kraniotis, P.R. Svennevig, K. Svidt, Improving building occupant comfort through a digital twin approach: A Bayesian network model and predictive maintenance method, Energy Build. 288 (Jun. 2023) 112992, https://doi.org/10.1016/j.enbuild.2023.112992.

[38] T. Østergård, R.L. Jensen, F.S. Mikkelsen, The best way to perform building simulations? One-at-a-time optimization vs. Monte Carlo sampling, Energy Build. 208 (Feb. 2020) 109628, https://doi.org/10.1016/j.enbuild.2019.109628.

[39] T. Onodera, K. Tamura, and K. Yasuda, "Integrated Optimization Using Global and Local Modeling," *Proc. ISCIE Int. Symp. Stoch. Syst. Theory Its Appl.*, vol. 2013, pp. 137–143, 2013, doi: 10.5687/sss.2013.137.

[40] R. Tong, et al., The construction dust-induced occupational health risk using Monte-Carlo simulation, J. Clean. Prod. 184 (May 2018) 598–608, https://doi.org/10.1016/j.jclepro.2018.02.286.

[41] A. Sorokin and I. Goryanin, "FBA-PRCC. Partial Rank Correlation Coefficient (PRCC) Global Sensitivity Analysis (GSA) in Application to Constraint-Based Models," *Biomolecules*, vol. 13, no. 3, Art. no. 3, Mar. 2023, doi: 10.3390/biom13030500.

[42] J.M. Lebreton, R.E. Ployhart, R.T. Ladd, A Monte Carlo Comparison of Relative Importance Methodologies, Organ. Res. Methods 7 (3) (Jul. 2004) 258–282, https://doi.org/10.1177/1094428104266017.

[43] D. Hou, I.G. Hassan, L. Wang, Review on building energy model calibration by Bayesian inference, Renew. Sustain. Energy Rev. 143 (Jun. 2021) 110930, https://doi.org/10.1016/j.rser.2021.110930.

[44] E.E. Broday, C.R. Ruivo, M. Gameiro da Silva, The use of Monte Carlo method to assess the uncertainty of thermal comfort indices PMV and PPD: Benefits of using a measuring set with an operative temperature probe, J. Build. Eng. 35 (Mar. 2021) 101961, https://doi.org/10.1016/j.jobe.2020.101961.

[45] S. Alghamdi, W. Tang, S. Kanjanabootra, and D. Alterman, "Effect of Architectural Building Design Parameters on Thermal Comfort and Energy Consumption in Higher Education Buildings," *Buildings*, vol. 12, no. 3, Art. no. 3, Mar. 2022, doi: 10.3390/buildings12030329.

[46] X. Chen, H. Yang, K. Sun, Developing a meta-model for sensitivity analyses and prediction of building performance for passively designed high-rise residential buildings, Appl. Energy 194 (May 2017) 422–439, https://doi.org/10.1016/j.apenergy.2016.08.180.

[47] S. Giorgi, M. Lavagna, K. Wang, M. Osmani, G. Liu, A. Campioli, Drivers and barriers towards circular economy in the building sector: Stakeholder interviews and analysis of five European countries policies and practices, J. Clean. Prod. 336 (Feb. 2022) 130395, https://doi.org/10.1016/j.jclepro.2022.130395.

[48] B. P. Raj *et al.*, "A Review on Numerical Approach to Achieve Building Energy Efficiency for Energy, Economy and Environment (3E) Benefit," *Energies*, vol. 14, no. 15, Art. no. 15, Jan. 2021, doi: 10.3390/en14154487.

[49] D. Popescu, S. Bienert, C. Schützenhofer, R. Boazu, Impact of energy efficiency measures on the economic value of buildings, Appl. Energy 89 (1) (Jan. 2012) 454–463, https://doi.org/10.1016/j.apenergy.2011.08.015.

[50] A. Horsley, C. France, B. Quatermass, Delivering energy efficient buildings: a design procedure to demonstrate environmental and economic benefits, Constr. Manag. Econ. 21 (4) (Jun. 2003) 345–356, https://doi.org/10.1080/0144619032000073505.

[51] Y. Lu, P. Li, Y.P. Lee, X. Song, An integrated decision-making framework for existing building retrofits based on energy simulation and cost-benefit analysis, J. Build. Eng. 43 (Nov. 2021) 103200, https://doi.org/10.1016/j.jobe.2021.103200.

[52] F. Asdrubali *et al.*, "An Evaluation of the Environmental Payback Times and Economic Convenience in an Energy Requalification of a School," *Buildings*, vol. 11, no. 1, Art. no. 1, Jan. 2021, doi: 10.3390/buildings11010012.

[53] P. Bragolusi, C. D'Alpaos, The valuation of buildings energy retrofitting: A multiple-criteria approach to reconcile cost-benefit trade-offs and energy savings, Appl. Energy 310 (Mar. 2022) 118431, https://doi.org/10.1016/j.apenergy.2021.118431.

[54] A. Sompolgrunk, S. Banihashemi, S.R. Mohandes, Building information modelling (BIM) and the return on investment: a systematic analysis, Constr. Innov. 23 (1) (Jan. 2021) 129–154, https://doi.org/10.1108/CI-06-2021-0119.

[55] N. Simões, M. Gonçalves, C. Serra, S. Resalati, Can vacuum insulation panels be cost-effective when applied in building façades? Build. Environ. 191 (Mar. 2021) 107602 https://doi.org/10.1016/j.buildenv.2021.107602.

[56] Q. He, S. T. Ng, M. U. Hossain, and M. Skitmore, "Energy-Efficient Window Retrofit for High-Rise Residential Buildings in Different Climatic Zones of China," *Sustainability*, vol. 11, no. 22, Art. no. 22, Jan. 2019, doi: 10.3390/su11226473.

[57] S. Burhenne, O. Tsvetkova, D. Jacob, G.P. Henze, A. Wagner, Uncertainty quantification for combined building performance and cost-benefit analyses, Build. Environ. 62 (Apr. 2013) 143–154, https://doi.org/10.1016/j.buildenv.2013.01.013.

[58] F. Branger, L.-G. Giraudet, C. Guivarch, P. Quirion, Global sensitivity analysis of an energy–economy model of the residential building sector, Environ. Model. Softw. 70 (Aug. 2015) 45–54, https://doi.org/10.1016/j.envsoft.2015.03.021.

[59] W. Tian, A review of sensitivity analysis methods in building energy analysis, Renew. Sustain. Energy Rev. 20 (Apr. 2013) 411–419, https://doi.org/10.1016/j.rser.2012.12.014.

[60] W.-H. Chen, et al., A comprehensive review of thermoelectric generation optimization by statistical approach: Taguchi method, analysis of variance (ANOVA), and response surface methodology (RSM), Renew. Sustain. Energy Rev. 169 (Nov. 2022) 112917, https://doi.org/10.1016/j.rser.2022.112917.

[61] "Norsk Norwegian price book - Økonomisk oppslagsverk - Norconsult Digital." Accessed: Apr. 18, 2024. [Online]. Available: https://norconsultdigital.no/produkter/norsk-Norwegian price book/.

[62] SN-CEN/TR 15459-2:2017, Energy performance of buildings - Economic evaluation procedure for energy systems in buildings - Part 2: Explanation and justification of EN 15459-1, Module M1-14, 2017, European committee for Standardization and European Free Trade Association (CEN/TR), Apr. 2017.

[63] "Tvedestrand videregående skole." Accessed: Jun. 16, 2024. [Online]. Available: https://tvedestrand.vgs.no/.

[64] "Byggteknisk forskrift (TEK10)," Direktoratet for byggkvalitet. Accessed: Sep. 29, 2024. [Online]. Available: https://www.dibk.no/regelverk/tek.

[65] NS 3701:2012, Kriterier for passivhus og lavenergibygninger Yrkesbygninger (Criteria for passive houses and low energy buildings Non-residential buildings), 2012, Norsk Standard.

[66] NS 3031:2014 Beregning av bygningers energiytelse er trukket tilbake, men vises fortsatt til i byggteknisk forskrift, 2014, Norsk Standard.

[67] J.-Y. Lee, P. Wargocki, Y.-H. Chan, L. Chen, K.-W. Tham, How does indoor environmental quality in green refurbished office buildings compare with the one in new certified buildings? Build. Environ. 171 (Mar. 2020) 106677 https://doi.org/10.1016/j.buildenv.2020.106677.

[68] D. Maulud and A. M. Abdulazeez, "A Review on Linear Regression Comprehensive in Machine Learning," *J. Appl. Sci. Technol. Trends*, vol. 1, no. 2, Art. no. 2, Dec. 2020, doi: 10.38094/jastt1457.

[69] R. Genuer, J.-M. Poggi, in: "random Forests", in *Random Forests with*, Springer International Publishing, Cham, 2020, pp. 33–55, https://doi.org/10.1007/978-3-030-56485-8_3.

[70] F. Zhang, L.J. O'Donnell, Chapter 7 - Support vector regression, in: A. Mechelli, S. Vieira (Eds.), Machine Learning, Academic Press, 2020, pp. 123–140, https://doi.org/10.1016/B978-0-12-815739-8.00007-9.

[71] A.C. Cinar, Training Feed-Forward Multi-Layer Perceptron Artificial Neural Networks with a Tree-Seed Algorithm, Arab. J. Sci. Eng. 45 (12) (Dec. 2020) 10915–10938, https://doi.org/10.1007/s13369-020-04872-1.

[72] M. Nalluri, M. Pentela, and N. rao Eluri, "A Scalable Tree Boosting System: XG Boost," p. 36, Jan. 2020, doi: 10.22259/2349-476X.0712005.

[73] "scikit-learn: machine learning in Python — scikit-learn 1.5.2 documentation." Accessed: Sep. 29, 2024. [Online]. Available: https://scikit-learn.org/stable/.

[74] "Introduction to TensorFlow," TensorFlow. Accessed: Sep. 29, 2024. [Online]. Available: https://www.tensorflow.org/learn.

[75] "Keras: The high-level API for TensorFlow | TensorFlow Core," TensorFlow. Accessed: Sep. 29, 2024. [Online]. Available: https://www.tensorflow.org/guide/keras.

[76] "XGBoost Python Package — xgboost 2.1.1 documentation." Accessed: Sep. 29, 2024. [Online]. Available: https://xgboost.readthedocs.io/en/latest/python/.

[77] "Introduction to Pandas and NumPy," Codecademy. Accessed: Sep. 29, 2024. [Online]. Available: https://www.codecademy.com/article/introduction-to-numpy-and-pandas.

[78] "Matplotlib — Visualization with Python." Accessed: Sep. 29, 2024. [Online]. Available: https://matplotlib.org/.

[79] "Seaborn." Accessed: Sep. 29, 2024. [Online]. Available: https://www.w3schools.com/python/numpy/numpy_random_seaborn.asp.

[80] F. M. Butt *et al.*, "Artificial Intelligence based accurately load forecasting system to forecast short and medium-term load demands," *Math. Biosci. Eng.*, vol. 18, no. 1, Art. no. mbe-18-01-022, 2021, doi: 10.3934/mbe.2021022.

[81] D. Chicco, M.J. Warrens, G. Jurman, The coefficient of determination R-squared is more informative than SMAPE, MAE, MAPE, MSE and RMSE in regression analysis evaluation, PeerJ Comput. Sci. 7 (Jul. 2021) e623.

[82] I. Tougui, A. Jilbab, J. El Mhamdi, Impact of the Choice of Cross-Validation Techniques on the Results of Machine Learning-Based Diagnostic Applications, Healthc. Inform. Res. 27 (3) (Jul. 2021) 189–199, https://doi.org/10.4258/hir.2021.27.3.189.

[83] A. Savine, "Sobol Sequence Explained by Antoine Savine," Medium. Accessed: Jun. 20, 2024. [Online]. Available: https://medium.com/@antoine_savine/sobol-sequence-explained-188f422b246b.

[84] D.S. Moore, G.P. McCabe, B.A. Craig, Introduction to the Practice of Statistics, Ninth edition, W. H. Freeman, New York, 2016.

[85] N. C. Gaitan, I. Ungurean, C. Roman, and C. Francu, "An Optimizing Heat Consumption System Based on BMS," *Appl. Sci.*, vol. 12, no. 7, Art. no. 7, Jan. 2022, doi: 10.3390/app12073271.

[86] W. Wu, H.M. Skye, P.A. Domanski, Selecting HVAC systems to achieve comfortable and cost-effective residential net-zero energy buildings, Appl. Energy 212 (Feb. 2018) 577–591, https://doi.org/10.1016/j.apenergy.2017.12.046.

[87] Q. Lu, G.A. Narsilio, G.R. Aditya, I.W. Johnston, Economic analysis of vertical ground source heat pump systems in Melbourne, Energy 125 (Apr. 2017) 107–117, https://doi.org/10.1016/j.energy.2017.02.082.

[88] M. A. Al-Ghamdi and K. S. Al-Gahtani, "Integrated Value Engineering and Life Cycle Cost Modeling for HVAC System Selection," *Sustainability*, vol. 14, no. 4, Art. no. 4, Jan. 2022, doi: 10.3390/su14042126.

[89] "NumPy -." Accessed: Sep. 30, 2024. [Online]. Available: https://numpy.org/.

[90] "pandas - Python Data Analysis Library." Accessed: Sep. 30, 2024. [Online]. Available: https://pandas.pydata.org/.

[91] W. Wu, H.M. Skye, Net-zero nation: HVAC and PV systems for residential net-zero energy buildings across the United States, Energy Convers. Manag. 177 (Dec. 2018) 605–628, https://doi.org/10.1016/j.enconman.2018.09.084.

[92] R. Bevans, "One-way ANOVA | When and How to Use It (With Examples)," Scribbr. Accessed: Jun. 17, 2024. [Online]. Available: https://www.scribbr.com/statistics/one-way-anova/.

[93] "Electricity prices," SSB. Accessed: Jun. 18, 2024. [Online]. Available: https://www.ssb.no/en/energi-og-industri/energi/statistikk/elektrisitetspriser.

[94] U. Çakır, K. Çomaklı, Ö. Çomaklı, S. Karslı, An experimental exergetic comparison of four different heat pump systems working at same conditions: As air to air, air to water, water to water and water to air, Energy 58 (Sep. 2013) 210–219, https://doi.org/10.1016/j.energy.2013.06.014.

[95] T. You, W. Wu, H. Yang, J. Liu, X. Li, Hybrid photovoltaic/thermal and ground source heat pump: Review and perspective, Renew. Sustain. Energy Rev. 151 (Nov. 2021) 111569, https://doi.org/10.1016/j.rser.2021.111569.

[96] R.R.R. Barbosa, R. Sadre, A. Pras, Difficulties in Modeling SCADA Traffic: A Comparative Analysis, in: N. Taft, F. Ricciato (Eds.), Passive and Active Measurement, Springer, Berlin, Heidelberg, 2012, pp. 126–135, https://doi.org/10.1007/978-3-642-28537-0_13.

[97] R. Krejčí, P. Čeleda, and J. Dobrovolný, "Traffic Measurement and Analysis of Building Automation and Control Networks," in *Dependable Networks and Services*, R. Sadre, J. Novotný, P. Čeleda, M. Waldburger, and B. Stiller, Eds., Berlin, Heidelberg: Springer, 2012, pp. 62–73. doi: 10.1007/978-3-642-30633-4_9.

[98] V. Heide, H. S. Thingbø, A. G. Lien, and L. Georges, "Economic and Energy Performance of Heating and Ventilation Systems in Deep Retrofitted Norwegian Detached Houses," *Energies*, vol. 15, no. 19, Art. no. 19, Jan. 2022, doi: 10.3390/en15197060.

[99] M. Miara, D. Günther, R. Langner, S. Helmling, J. Wapler, 10 years of heat pumps monitoring in Germany. Outcomes of several monitoring campaigns. From low-energy houses to un-retrofitted single-family dwellings. In *12th IEA Heat Pump Conference*, 2017.

[100] A. O'Donovan, P. O'Sullivan, In-Use Performance of Air-to-Water Heat Pumps: are the Standards robust? E3S Web Conf. 246 (2021) 06002, https://doi.org/10.1051/e3sconf/202124606002.

[101] G. Zhou, H. Moayedi, L.K. Foong, Teaching–learning-based metaheuristic scheme for modifying neural computing in appraising energy performance of building, Eng. Comput. 37 (4) (Oct. 2021) 3037–3048, https://doi.org/10.1007/s00366-020-00981-5.

[102] M. Ilbeigi, M. Ghomeishi, A. Dehghanbanadaki, Prediction and optimization of energy consumption in an office building using artificial neural network and a

genetic algorithm, Sustain. Cities Soc. 61 (Oct. 2020) 102325, https://doi.org/10.1016/j.scs.2020.102325.

[103] M. Aminpour, R. Alaie, N. Kardani, S. Moridpour, M. Nazem, Highly efficient reliability analysis of anisotropic heterogeneous slopes: machine learning-aided Monte Carlo method, Acta Geotech. 18 (6) (Jun. 2023) 3367–3389, https://doi.org/10.1007/s11440-022-01771-7.

[104] G. Kalogeras, S. Rastegarpour, C. Koulamas, A.P. Kalogeras, J. Casillas, L. Ferrarini, Predictive capability testing and sensitivity analysis of a model for building energy efficiency, Build. Simul. 13 (1) (Feb. 2020) 33–50, https://doi.org/10.1007/s12273-019-0559-8.

[105] L. Hu, V. N. Nair, A. Sudjianto, A. Zhang, and J. Chen, "Interpretable Machine Learning based on Functional ANOVA Framework: Algorithms and Comparisons," arXiv.org. Accessed: Oct. 17, 2024. [Online]. Available: https://arxiv.org/abs/2305.15670v1.